UNIVERSITÀ DEGLI STUDI DI SASSARI

Scuola Internazionale di Dottorato in Scienze Biomolecolari e Biotecnologiche
International PhD School in Biomolecular and Biotechnological Sciences
(*Cycle XXVI*)
Curricula Biochemistry, Physiology and Molecular Biology

Director: Prof.ssa Claudia Crosio

Characterisation of molecular and phenotypic effects induced by Gestational Diabetes Mellitus (GDM) on endothelial cells and placenta tissue

Tutor: Prof. Gianfranco Pintus

Co-tutor: Prof.ssa Costanza Emanueli

***Dottorando*/PhD student: Dr.ssa Ilaria Floris**

La presente tesi è stata prodotta nell'ambito della scuola di dottorato in Scienze Biomolecolari e Biotecnologiche dell'Università degli Studi di Sassari, a.a. 2010/2011 – XXVI ciclo, con il supporto di una borsa di studio finanziata con le risorse del P.O.R. SARDEGNA F.S.E. 2007-2013 - Obiettivo competitività regionale e occupazione, Asse IV Capitale umano, Linea di Attività l.3.1.

INDICE

ABSTRACT

Gestational diabetes mellitus (GDM) is characterised by maternal hyperglyceamia first recognised during pregnancy. GDM produces chronic foetal hyperglyceamia and expressional changes in foetal endothelial cells (ECs).
Epigenetic modulation of foetal endothelial genes by the intra-uterine environment has been proposed. MicroRNAs (miRs) inhibit the expression of their mRNA targets and have been implicated in diabetes-induced endothelial dysfunction. MiR-101 impairs EC in part via direct inhibition of the methyltransferase Enhancer of Zester Homolog2 (EZH2) which catalysed the trimethylation on lysine 27 of histone H3 (H3K27m3).
We aimed to characterize the molecular and functional impact of GDM on the foetal ECs derived from the umbilical cord vein (HUVECs).
HUVECs prepared from GDM or healthy pregnancies, were assessed for apoptosis, migration, and angiogenic capacity. GDM-HUVECs showed decreased functional capacities, increased miR-101, reduced EZH2 and H3K27m3 expression. In GDM-HUVECs, miR-101 inhibition increased EZH2 expression, improved survival and endothelial functions. Moreover, cultured healthy-HUVECs were exposed to high (25mM, HG) or normal (5mM) D-glucose concentrations for 48 hours before being assessed for the aforementioned assay and for miR-101 and EZH2 expression. Similarly to GDM, *in vitro* HG impaired healthy-HUVEC function and elicited a concomitant increased in miR-101.
In conclusion GMD and HG impair HUVEC functions in part also via miR-101 upregulation.

ABBREVIATIONS

Gestational Diabetes Mellitus (GDM)

Diabetes Mellitus (DM)

Cardiovascular diseases (CVD)

Micro-RNAs (miRs)

Enhancer of Zester Homolog 2 (EZH2)

Policomb Repressor Complex 2 (PRC2)

Human umbilical vein endothelial cells (HUVEC)

HUVECs extracted from healthy mothers (Ctr-HUVECs)

HUVECs extracted from gestational diabetic mothers (GDM-HUVECs)

Tri-methylation of histone H3 on Lysine 27 (H3K27m3)

Foetal bovine serum (FBS)

Conditioned medium (CM)

Chromatin immunoprecipitation (CHIP)

SiRNA-mediated knock down of EZH2 (EZH2-siRNA)

SiRNA-control (siRNA-Ctr)

High Glucose (HG)

1. INTRODUCTION

1.1 Gestational Diabetes Mellitus

Gestational diabetes mellitus (GDM) is a syndrome characterised by glucose intolerance leading to maternal hyperglyceamia first recognized during pregnancy *[1]*.

Approximately 7% of pregnancies are complicated by gestational diabetes mellitus (GDM) (ranging from 1 to 14%, depending on the population studied and the diagnostic tests employed) *[2]*.

In GDM condition, the maternal hyperglyceamia leads to foetal hyperinsulinemia and may be responsible for adverse long-term maternal and foetus outcomes: high risk for developing type 2 diabetes mellitus (DM) and cardiovascular diseases (CVD), atherosclerosis, increased perinatal morbidity (e.g. macrosomia, birth trauma, pre-eclampsia), and long-term consequences in offspring (e.g. childhood overweight, metabolic diseases that may increase risk of CVD and diabetes) *[3]*.

The molecular mediators and signalling pathways from the mother to the developing foetus, involved in the program of the metabolic phenotype are not fully elucidated. There are evidences explaining that in diabetic condition, the high amount of maternal D-glucose can cross the placental barrier becoming available to the fetus, while maternal insulin does not cross the placenta, establishing chronic foetal hyperglyceamia. In fact, the developing foetal pancreas responds to an increased D-glucose load by increasing synthesis and release of insulin, which acts as a foetal growth hormone. This is the basic concept of the "Pedersen's hyperglyceamia-

hyperinsulinism hypothesis", where fetal overgrowth due to hyperinsulinemia in response to increased transplacental D-glucose transfer is proposed, as recently reviewed *[4]* (**Fig.1**) explaining observations showing that offspring of diabetic mothers exhibit abnormal growth of the foetus (macrosomia) and high birth weight *[5]*. Moreover, the altered insulin signalling causes alterations in the physiology of the placenta, hormone-induced dysfunction that could lead to the observed perinatal complications *[6, 7, 8]*. Further analysis expanded this theory, also other insulin secretagogues alterations, including free fatty acids, ketone bodies, and amino acids can contribute to the severity of the outcomes *[9]*.

The clinical manifestations of GDM have been attributed mainly to the condition of hyperglycaemia, hyperinsulinemia, hyperlipidaemia, and foeto-placental endothelial dysfunction *[10, 11]*.

1.2 Endothelial Dysfunction in Gestational Diabetes Mellitus

In GDM, various organs show structural and functional alterations, including endothelial dysfunction of the foeto-placental micro- and macro-circulation *[12, 13]*.

As early as in 1980 is known that maternal diabetes during pregnancy affects infant vasculature. Asmussen studied the umbilical vessels of infants born to women with type1 diabetes mellitus (T1DM) observing that the umbilical vessels showed pathological changes with early atherosclerosis, including focal intimal thickening and glycogen accumulations in the cells of

the intima and the media *[14]*. These altered metabolic phenotypes could partially be explained by the involvement of multiple mediators, a multifactorial contribution of nutrient- (e.g. D-glucose, fatty acids, aminoacids) and hormone- (e.g. insulin, leptin) triggered signals between the mother and the developing foetus. Also several inflammatory cytokines levels are elevated in diabetic and gestational diabetic mothers *[15]*, and in obese pregnant women *[16]*. These changes in inflammatory cytokines are proposed as contributors and potential mediators of metabolic programming. Impairment of endothelial function often occurs prior to diagnosis of diabetes mellitus (DM) *[17]*, and endothelial dysfunction is often present years before any signs of apparent microangiopathy *[18]*. Such findings have generated the hypothesis that, in diabetes, endothelial dysfunction may precede the development of chronic hyperglyceamia, encouraging the idea that the next generation of therapeutic agents should also focus on the mechanisms of endothelial dysfunction, and not only on glyceamic control *[19]*.

A recent study has tested whether biomarkers of endothelial dysfunction may be altered in women with GDM and their foetuses. Has been demonstrated an increase in circulating adhesion molecules in patients with GDM. Moreover, GDM subjects had significantly decreased circulating Endothelial Progenitor Cell (EPC) counts in maternal blood, decreased Superoxide Dismutase (SOD) isoforms mRNA expression in both maternal and cord blood, and increased Endothelial NOS (eNOS) mRNA expression in both maternal and cord blood *[20]*. These findings are consistent with the

hypothesized mechanisms where hyperglycemia can lead to increased oxidative stress and endothelial dysfunction in diabetes. Importantly, these results suggest that alterations in endothelial function are present in both mothers and their fetuses in GDM pregnancies. Increased nitric oxide (NO) synthesis has also been reported in human placental veins and arteries *[21]* and in primary cultures of HUVEC isolated from pregnancies with GDM *[22, 23]*.

If these measures remain elevated, it is possible that these alterations can confer an increased risk for the development of CVD, atherosclerosis and type 2 DM.

1.3 The '*Glyceamic Memory*' theory

Clinical trials of diabetes patients (type 1 and 2) accent the importance of early and intensive treatment finalized to a good glyceamic control and bring attention to the prolonged damage of hyperglycemia on various organs. A good glyceamic control is recognised as an important component in the clinical treatment of diabetes. The strategies based on intensive blood-glucose-lowering have confirmed the clinical relevance of strict metabolic regulation to attenuate diabetic vascular complications *[24, 25, 26]*.

The concept of 'metabolic or glycemic memory' started more than 20 years ago, where epidemiological studies demonstrated that, despite stringent long-term glycemic control, the previous hyperglyceamia affects the vasculature leading persistent alterations *[24, 25, 26]*. Even experimental

studies on animal models had suggested that prior hyperglycemia induces memories affecting endothelial cells with persistent effects, which may be responsible for the development of chronic vascular complications associated with diabetes *[27, 28]*.

Recently, strong experimental evidences support the role of gene-regulating events conferred by hyperglyceamia on the development and persistence of vascular complications due to diabetes. These heritable gene-alterations have been associated with deregulation at level of epigenome (chromatin histone modifications, DNA methylation). In fact, glucose-mediated chromatin and transcriptional changes has been found in vascular cells cultured in high glucose, in association with persistent inflammation *[29, 30, 31]*. These *in vitro* studies have opened the possibility that similar mechanisms may operates also in the microvasculature.

A better understanding of the molecular events and transcriptional gene-regulation mediated by chromatin modification will help to identify novel approaches to inhibit, attenuate, or reverse the persistent deleterious consequences of diabetes.

1.4 The role of microRNAs in endothelial dysfunction

MicroRNAs (miRNAs) are small non coding RNA molecules (~22 nucleotide) able to modulate many molecular pathways involved in both physiological and pathological process acting on target gene: inhibiting the mRNA translation and/or causing its degradation *[32]*.

The first study describing miRNAs involvement in endothelial cells exposed to high glucose is Wang *et al [33]*. They found elevated miR-320 levels in ECs derived from diabetic rats, accompanied by decreased proliferation and migration. After, many other authors have increased the number of miRNAs involved in hyperglyceamia, diabetes, angiogenesis and endothelial dysfunction. MiRNAs can have a protective and pro-angiogenic effect or exert a deregulation/inhibition of angiogenesis, contributing to the development of vascular complication (**Table I**).

1.5 The epigenetic regulator Enhancer of Zester Homolog2 (EZH2) and its role in endothelial dysfunction

The protein Enhancer of Zester Homolog2 (EZH2) is a well-characterized regulator of the epigenome, it functions as a histone methyltransferase in the Policomb Repressor Complex2 (PRC2), which contains EED, SUZ12, and other proteins *[34]*. PRC2 initiates and maintains the methylation of histone H3 on Lysine 27 (H3K27). The epigenetic mark H3K27m3 mediates the long term epigenetic gene silencing *[34]*. In fact, according to the 'histone code' hypothesis, histone marks are deposited by 'writer' proteins as EZH2 and recognized by 'reader' proteins, that together with chromatin regulators trigger the transition between open (permissive) or close (non-permissive) chromatin, regulating gene transcription (**Fig.2**). PRC2, like other epigenome regulators, works in complex. It's physically and functionally linked with histone deacetylases (HDACs), with histone methyltransferase

(HMTs) *[35]*, and other proteins. In particular, one of them is the Jumonji domain family histone H3K36me2 and H3K4me3 demethylase KDM2B (or NDY/FBXL10/JHDM1B) *[36]*, which play a central role in the 'repressive histone code' by removal of the active marks H3K36m2 and H3K4m3. The functional interaction between EZH2 and KDM2B is not completely elucidated, even though has been showed that they are coordinately down-regulated in a series of primary cells undergoing senescence *[37]*.

Again, it has been shown that EZH2 is involved in the maintenance of pluripotency in human stem cells *[38, 39]*, but little is known about its function in differentiated cells.

However, recent studies have suggested a physiological role for EZH2 in endothelial function, mediated by miR-101. The authors identified a pro-angiogenic VEGF/miR-101/EZH2 axis, providing evidence for a functional link between: growth factor-mediated signaling, post-transcriptional silencing through miR-101 on its target gene EZH2, epigenetic modifications through histone-methylation, and the angiogenic process *[40, 41].*

Currently, has been identified the role of EZH2 in endothelial cells using knockdown (KD) strategy. The authors have reported 946 Ezh2 target genes regulated by more than 2-fold change; almost two thirds of the genes were up-regulated after EZH2 KD, which is in accordance with its repressive function. Having identified genes that contain the histone modification H3K27m3 and genes regulated on the mRNA level by EZH2 silencing, in endothelial cells, they could identify direct EZH2 target genes. Basically, they combined the results of the ChIP-on-chip with the EZH2 knockdown

expression arrays. Some of the putative target genes identified are known to play a role in the regulation of vascular cell proliferation, spreading, and angiogenesis, such as fibroblast growth factor 1 (FGF-1), cadherin-13, disintegrin and metalloproteinase domain 12, frizzled homolog 7, transforming growth factor-α (TGF-α), hairy/enhancer of-split related with YRPW motif 2, and versican. In addition, other EZH2 target genes were already implicated in endothelial dysfunction and cardiovascular disease such as interleukin-1ß (IL-1ß), insulin-like growth factor-2 (IGF-2), bone morphogenetic protein receptor-1A (BMPR-1A), spondin-1 (SPON-1), interleukin-11 (IL-11), inducible nitric oxide synthase (iNOS), transforming growth factor-ß–induced gene (TGFßI), and insulin receptor substrate-1 (IRS-1) *[42].*

1.6 FGF2 or VEGF/KDM2B/EZH2/miR-101/EZH2 axis

The FGF-2-KDM2B/EZH2-miR-101-EZH2 axis, firstly studied in tumor cells, and documented also in primary fibroblasts in culture *[36]*, has been recently analysed in endothelial cells as one of the pathways activated in response to VEGF *[40, 41]*, as mentioned before.

Pathologically, what it's known is that EZH2 overexpression, common in both hematopoietic malignancies and solid tumors, promotes cell proliferation, migration and invasiveness. Moreover, the overexpression of EZH2 in the tumor stroma stimulates angiogenesis *[38, 41, 43],* while the pharmacologic disruption of the EZH2-containing PRC2 complex induces

apoptosis in cancer cells and increase the sensibility to the radiation *[44].* The high EZH2 levels in tumor cells are associated with the down-regulation of miR-101, which targets EZH2 *[40, 41, 45, 46]*. The repression of miR-101 is the result of chromatin modifications induced by histone demethylase KDM2B (or NDY1) on specific regulatory region of *miR-101 locus [45]*. The upregulation of KDM2B in these tumors is cell autonomous; it's driven by growth factor signals, like fibroblast growth factor-2 (FGF-2) and (VEGF) via CREB phosphorylation and activation, downstream of the DYRK1A kinase. The upregulation of KDM2B triggers the recruitment of basally expressed EZH2, which binds and represses the *miR-101 locus* in concert with NDY1. The repression of miR-101 leads to the upregulation of EZH2, which in addition to its direct effects on gene expression, stabilizes the NDY1-initiated repression of miR-101, and regulates miR-101 target genes. (**Fig. 3**) *[45].*

Cancer is another pathology directly dependent on angiogenesis and it is not surprising that diabetes is positively correlates with hepatic, pancreatic, colon, endometrial, breast, and bladder cancer incidence and prognosis *[47, 48]*, but negatively with prostate cancer *[49, 50]*. Thus, both angiogenesis in organs and tumour growth are regulated in a tissue-specific manner in patients with diabetes. Similar to the mechanisms of diabetic tissue-specific aberrant angiogenesis, the molecular mechanisms of positive or negative tissue-specific associations of tumour growth and diabetes are unknown.

1.7 Placenta

The human placenta is the highly specialised organ supporting the normal growth and the development of the foetus. The placenta provides oxygen and nutrients to the foetus, while eliminate carbon dioxide and other waste products. The placenta can help to protect the foetus against certain xenobiotic molecules, infections and maternal diseases, furthermore, can release hormones into both the maternal-foetal circulation to affect pregnancy, metabolism, foetal growth, parturition and other functions.

The main functional units of the placenta are the chorionic villi, which gradually branched into smaller intermediate and terminal villi. The villi are surrounded mainly by a syncytiotrophoblast layer in which the nuclei are often grouped together to form syncytial knots. The maternal blood circulate in the intervillous space, while the foetal blood is separated from maternal blood by only three or four cell layers (placental membrane) in the surrounding intervillous space. The centre of the villi contained loose mesenchymal tissue with fibroblasts, macrophages and blood vessels. (**Fig.4**)

1.8 Placental dysfunction in Gestational Diabetes Mellitus

In GDM mothers, the increases in circulating glucose concentration may affect the placental angiogenesis.

During the entire gestation, maternal and foetal tissues interact to establish an appropriate vascularization in the placental decidua and chorion. Decidual angiogenesis involves proliferation, migration and maturation of

maternal and foetal endothelial cells. An increase in glucose can affect the endothelial physiology, compromising the placental angiogenesis, function and the foetal development *[51, 52]*.

The chronic maternal and foetal hyperglyceamia can promote atherosclerosis and consequent hypoxia/ischemia with problem in blood flow, increases in syncytial knots and in fibrin deposition. Hyperglyceamia has been also associated with higher deposition of the extracellular vascular amyloid, which consists on a heterogeneous mix of fibrillar proteins *[53, 54]*. The production of these proteins may explain the appearance of more condensed mesenchyme around blood vessels.

In addition to amyloid deposition, hyperglyceamia also causes exacerbated collagen production by the vascular endothelium. A study indicate that the accumulation of collagen in the tunica media of vessels in intermediate villi and in stromal villi depend on the extent of the glucose alterations *[55]*.

2. MATERIALS AND METHODS

Human umbilical cords and study groups

Umbilical cords were collected after delivery from 24 full-term normal or 22 full-term gestational diabetic pregnancies (**Table I**). The investigation conforms to the principles outlined in the Declaration of Helsinki. Ethics Committee approval from the Faculty of Medicine of the University of Sassari and patient informed consent were obtained. Patients with basal glycaemia 90 mg/dL (i.e. overnight starvation) and 140 mg/dL at 2 h after an oral glucose load (75 g) were diagnosed as gestational diabetes (**Table II**).

Human endothelial cells extraction

Primary endothelial cells (HUVECs) obtained from healthy and gestational diabetic mothers were extracted from umbilical cord vein. Umbilical cord vein were washed in PBS and gently massed to push the blood out. The ECs were detached from the lumen of the vein by treatment with collagenase. The incubation were performed for 10 min at 37°C with 0.05% (w/v) collagenase type II from Clostridium hystolyticum (Sigma) in medium M199 (Invitrogen) containing 100 U/ml of penicillin G sodium salt and 100µg/ml streptomycin sulfate (Sigma). Then, the cellular suspension has been collected and centrifuged at 1000×g for 10 min. The ECs were resuspended in 5 ml of medium M199 supplemented with 10% (v/v) foetal calf serum (FCS), 10% (v/v) newborn-calf serum (Invitrogen, Carlsbad, CA), 2mM glutamine and antibiotics, then plated in 25 cm2 tissue culture flasks (Falcon, Oxnard, CA)

pre-treated with 0.1 % gelatin and cultured in an atmosphere of 5% CO2/95% air.

The human cells were extracted in the University of Sassari, kept in culture until passage two, then stored and imported for research at the University of Bristol following ethical approval (NRES/REC reference: 12/WM/0366 for the IRAS protocol 113869).

Cell culture

Primary endothelial cells (HUVECs) obtained from healthy and gestational diabetic mothers, were cultured in EGM2 medium (Lonza) with 10% FBS (foetal bovine serum). The cellular purity was tested by FACS using CD31 (1:100) as endothelial marker (**Fig. 5**).

High Glucose experiments

The HUVECs obtained from healthy donors were cultured in high D-glucose (SIGMA) to mimic the hyperglycaemic conditions choosing two different final concentrations: 12.5mM and 25mM. L-glucose (SIGMA) has been used to make the osmotic control for each condition, adding L-glucose to the EGM2 up to raise the same final concentration of D-glucose. The time-points of treatment are: 12 – 24 - 48 hours. For each time-point the cells has been analysed in their phenotypic properties with functional assays in association with mRNA, microRNA and proteins levels analysis.

HUVECs functional assay

The HUVECs has been analysed for their endothelial phenotypic properties with functional assays to characterise:

- the effects of high glucose *in vitro*;
- the phenotype of the HUVECs extracted from gestational diabetic mothers compared to the lineages extracted from 'healthy' mothers donor.

1. BrdU incorporation assay was used to test the proliferative capacity of the HUVECs. The assay was performed in a 96-well format using a commercially available colorimetric enzyme-linked immunosorbent assay kit (ROCHE). To test the effects of the high D-glucose, 150.000 cells/well has been placed in a 6-well plate then, after 12 – 24 – 48 hours and 6 days of treatment, trypsinized and plated in the 96-well for the assay (2000 cells/well); after 24 hours of BrdU incorporation the cells were fixed and analysed. The index of proliferative capacity in response to FBS, has been calculated firstly maintaining the HUVECs for 1 hour without FBS then, culturing each lineage with 0.5% FBS and with 10% FBS for 24 hours, in presence of BrdU. Then, fixed the cells and performed the BrdU assay. The ratio between the average of proliferative capacity of cells cultured with 0.5% FBS and the average of proliferation occurred with 10% FBS, could gave us the increment of proliferation in response to FBS, after strong serum starvation.

2. Scratch assay was assessed to test the effect of high glucose on the migration capacity. The cells were cultured in a 12-well plate (30.000 – 50.000 cells/well) and treated with D-glucose (and L-glucose) for 12 – 24 – 48 hours and 6 days. Then, in the monolayer has been made manually the scratch with pipette tip, changed the medium with fresh EGM2 (10% FBS) adding 2mM hydroxyurea (SIGMA) to induce growth arrest. Images were taken at 0, 6 and 10 hours at 5X using a Brightfield inverted microscope. The wound area was measured using ImageJ software (NIH) and normalized to time 0 wounds to calculate the velocity of closing scratch in the first 6 and 10 hours; the final value has been obtained as the average between the velocity of closing scratch at 6th and 10th hour.

3. The angiogenic capacity has been tested with the **matrigel assay**, using the Matrigel matrix (BD Matrigel basement membrane complex) as substrate for the successful endothelial cell tube formation and allows the study of angiogenesis *in vitro*. The cells, followed the high glucose treatment, or transfection, has been placed on matrigel (15.000 cells/well on 40 µl of already solidified matrigel, in triplicate, using 96-well format). The images were taken after 6 and 24 hours at 5X using a Brightfield inverted microscope. The total length of tubes (mm) has been calculated as parameter of angiogenic capacity *in vitro*.

4. The apoptosis has been studied by the kit **Cell Death Detection ELISA** (ROCHE).

D-glucose treated cells, after 24 – 48 hours and 6 days were used for the ELISA (100.000 cells/per condition). The ELISA is specific to detect the mono- and oligo- nucleosome in the cytoplasmic fraction of the cells lysate. In fact, apoptosis is accompanied by membrane blebbing, condensation of cytoplasm and activation of endogenous endonuclease. The enrichment of mono- and oligo- nucleosomes in the cytoplasm of the apoptotic cells is due to the DNA degradation and occurs several hours before the plasma membrane breakdown. For the ELISA assay, the cellular pellet has been incubated with the Incubation Buffer furnished by the kit for 30 minutes; then centrifuged at 20.000 g for 10 minute to obtain the cytosolic fraction in the supernatant. It has been collected and used for the photometric enzyme immunoassay. The values of absorbance have been reported in fold change.

Conditioned Medium preparation

HUVECs from 'healthy' and GDM mothers (N=4) were cultured in 6well-plate (150.000 cells/well), then starved strongly for 1 hour in EGM-2 without FBS. Thereafter, media was replaced with 0.5%FBS and cells were incubated for another 24 hours. Subsequently, conditioned media was collected, centrifuged and stored at −80°C until further analysis.

ELISA

We measured secreted FGF2 (or basic FGF) and VEGF ($VEGF_{165}$, $VEGF_{121}$, $VEGF_{165b}$) in the conditioned medium samples using the Duo Set ELISA Development kit (human VEGF Duo Set, R&D Systems; Minneapolis, MA,

USA). ODs were measured at 450–570 nm and FGF2 or VEGF was calculated as cell number adjusted amount (ng/ml) according to the standards used. The EGM-2 media with 0.5% serum served has been used as negative control.

Transfection

12.5nM of scramble control (Ambion), pre-miR-101 (Ambion), anti-miR-101 (Ambion), EZH2 siRNA (Qiagen) or siRNA-AF (Qiagen) oligonucleotides were transfected into HUVECs using Lipofectamin2000 (Invitrogen), according the manufacturer's protocol. After 5 hours, the transfection medium was replaced by EGM2 (10% FBS) until further analysis.

mRNA and miRNAs RT-PCR analysis

Total RNAs were isolated by TRizol method, and reverse transcription was performed using the QIAGEN QuantiTect Reverse Transcription kit, according to the manufacturer's protocol.

MRNA levels of EZH2, KDM2B, VEGF-A have been analysed. Their levels normalized to beta actin, chosen as housekeeping gene.

For miRNAs analysis, reverse transcription was performed using the TaqMan MicroRNA Reverse Transcription kit (Ambion), Real-time PCR was performed using the TaqMan universal master mix in the Light- Cycler480 qPCR detection system (Roche). Primers for RT and qPCR were included in TaqMan MicroRNA assays from Ambion (see online supplement). RNU6B was used as a reference for normalization.

Relative levels of mRNA and miRNAs were defined from threshold cycle (Ct) values calculated by the $2^{-\Delta\Delta Ct}$ method.

Western Blot assay

Total protein or nuclear protein fraction extracted from HUVECs were loaded, subjected to SDS–PAGE and blotted on PVDF membranes.

For the total lysate, cells were washed in cold PBS and lysate with RIPA buffer (150mM sodium chloride, 1.0% Triton X-100, 0.5% sodium deoxycholate, 0.1% SDS-sodium dodecyl sulphate, 50mM Tris, pH 8.0) supplemented with protease inhibitors (1mM DTT, 0.5mM PMSF, 2 ul/ml Protease Inhibitors Cocktails, Sigma).

For the nuclear/cytoplasmic protein separation, has been followed the protocol: briefly, cells were washed twice with cold PBS then resuspended in buffer A (10mM Hepes pH 7.5, 10mM KCl, 1.5mM MgCl2, 0.34M Sucrose, 10% Glicerolo, 0.1% TritonX-100) supplemented with protease inhibitors (1mM DTT, 0.5mM PMSF, 2 ul/ml Protease Inhibitors Cocktails, Sigma) and incubated at 4ºC on a rotator for 30 minutes to help the lysis. By centrifuging at 6500×g for 5 minutes at 4 °C nuclei were isolated, washed once with buffer A (depleted of Triton X-100) and subsequently resuspended in buffer B (3mM EDTA, 0.2mM EGTA, plus protease inhibitors, as buffer A). Blots were incubated over night at 4°C with primary antibodies against EZH2 (Active Motif, 1:2000); anti-trimethyl-Histone H3 (Lys27) (UPSTATE Cell Signaling, 1:2000); alpha/beta tubulin (Cell Signaling, 1:2000), actin (Santa Cruz, 1:1000); anti-Histone H3 (Active Motif, 1:2000); anti-LaminA/C

(Active Motif, 1:1000) and an HRP-conjugated secondary antibody, followed by chemiluminescence detection. Levels were visualized on X-ray film (GE healthcare) and quantified using ImageJ software (NIH Image).

ChIP

Chromatin immunoprecipitation (ChIP) assays were performed using gestational diabetic and 'healthy' HUVECs or 'healthy' HUVECs exposed to normal and high D-Glucose concentration (respectively 5mM and 25mM). Cells were fixed in 1% formaldehyde/PBS; after 10 minute of incubation at RT, the cross-linking has been stopped by adding glycine to a final concentration of 0.125M. The cells were washed in PBS and harvested in SDS buffer (100mM NaCl, 50mM Tris-HCl (pH 8), 5mM EDTA (pH 8), 0.2% NaN3, SDS 0.5%). The chromatin pellet has been obtained by centrifuging 6 min at 1200 rpm at 4°C. The only surnatant kept and resuspended to the final volume of 300 µl with ice-cold IP Buffer (= 1 vol of SDS Buffer : 0.5 vol Triton Diluition Buffer). Triton Diluition Buffer made with 100mM Tris-HCl (pH 8.6), 100mM NaCl, 5mM EDTA (pH 8), 0.2% NaN3, 5% Triton-X100. The chromatin were sonicated and then incubated with magnetic beads and specific antibodies against EZH2 (mouse monoclonal, Active motif, Lot 2023363) and control IgGs. Aliquots of immunoprecipitated DNAs were analyzed in triplicate by real-time quantitative PCR with the primers specific for the promoter region of miR-101 gene. Enrichment (n-fold) of target genomic regions immunoprecipitated by each specific antibody was normalized to the levels obtained with species-matched control IgGs and

plotted as the increase over the level of enrichment at the negative-control region.

Immunohistochemistry

After fixation, the human placental samples from 'healthy' and GDM mothers (N=2), were washed in PBS and processed for embedding in paraffin. Deparaffinized sections 5 mm thick were stained with hematoxylin-eosin to identify the villous and the decidual placental regions. Samples from two different paraffin blocks of each placenta were analyzed.

Picrosirius Red staining

Hyperglycemia can lead to the exacerbated production of collagen by the vascular endothelium. To assess collagen production by placental tissue, 5 mm-thick sections were stained with Picrosirius Red, which allows the visualization of collagen fibers by light microscopy (red staining) or polarized light microscopy *[54]*. After deparaffinization, the sections were stained with 0.1% Picrosirius Red in a saturated solution of picric acid for 20 minutes.

Statistical analysis

Data are expressed as means ± SEM from at least three independent experiments. Differences between D-glucose treated HUVECs compared to normal glucose-controls or between gestational diabetic compared to 'healthy' HUVECs were tested using unpaired Student's t test, just if the

Normality test has been passed, otherwise using the Mann-Whitney Rank Sum Test. Statistical analyses were performed using GraphPad Prism version 5.0 and SigmaStat 3.1; P values < 0.05 were considered statistically significant. Pearson's correlation and respective p value has been calculated with GraphPad Prism.

3. RESULTS

3.1 Gestational diabetes induces long term phenotypic alterations on HUVECs

The characteristic of the donor mothers is presented in **Table II**. The HUVECs has been extracted from 'healthy' (Ctr-HUVECs) and gestational diabetic mothers (GDM-HUVECs), as described in the protocol. The purity of the cells has been investigated by FACS using the endothelial marker CD-31. As the figure **Fig. 5** shows, both GDM-HUVECs and Ctr-HUVECs are CD-31 positive (>95%).

It was already shown that endothelial cells isolated form diabetic donors conserve a 'glyceamic memory' in culture *[55]* suggesting that long-term chronic hyperglyceamia induce persistent outcomes. In fact, in comparison with 'healthy' controls, GDM-HUVECs showed reduced capacity to form cellular network on Matrigel (**Fig. 6**); a lower proliferative index after stimulation with foetal bovine serum (FBS) (**Fig. 7**); impaired migration capacity (measured in 'scratch assays') (**Fig. 8**); and increased apoptosis (**Fig. 9**). In our study the findings are consistent with the hypothesized mechanisms where hyperglyceamia leads to endothelial dysfunction due to diabetes. Moreover, the observed endothelial cell phenotype were present after five-six passages in culture in normal D-Glucose condition and represents long-term effect of maternal GDM environment *in utero*. Our study is in line with the 'glyceamic memory' theory, where previous

hyperglycaemia confers persistent effects on vasculature, even if returned to normal glucose levels.

3.2 MicroRNA expressional analysis in GDM-HUVECs and Control-HUVECs

In association with the phenotypic characterisation, the HUVECs from 'healthy' and from GDM mothers has been screened for the microRNAs belonging to the extended miR-16 family (miR-15a, miR-15b, miR-16, miR-103, miR-107, miR-195, miR-424 and miR-497, miR-503), already involved in diabetes and its vascular complications *[56, 57, 58]*, and for microRNA-101, which was previously shown to inhibit angiogenesis by targeting the epigenetic enzymes EZH2 *[40, 45, 46]*. As shown in **Fig. 10**, a pilot expressional screening using n=8 samples per group showed no statistical significant differences in the miRs levels, but a trend toward increased levels in the GDM-HUVECs compared to the 'healthy' HUVECs. The miR-101 data was assessed with a larger number of samples (n=18), and we found higher levels in the GDM-HUVECs compared with the controls ($P<0.05$) (**Fig.11a, b**). Moreover, we found very high positive Pearson's correlation between miR-101 levels and the apoptosis measured in 'healthy' and GDM-HUVECs (Pearson $r = 0.9$, $P<0.001$) (**Fig.12**).

3.3 Gestational diabetes induces changes in the components of the FGF2-VEGF/KDM2B/EZH2-miR-101-EZH2 axis

GDM reportedly can induce epigenetic changes at the level of DNA methylation in various foetal organs *[59]*, including the placenta *[60]*. In our study, in association with the higher miR-101 levels (**Fig. 11a, b**), the epigenetic histone methyltransferase EZH2 were found lower in GDM-HUVECs compare with the 'healthy' HUVECs lineages ($P<0.05$), both in mRNA (**Fig.11 c, d**) and in protein levels (**Fig.11f**). Moreover, **Fig.11e** shows the negative Pearson's correlation found between miR-101 levels and EZH2 mRNA levels, confirming previous reports which have validated EZH2 as a target-gene of miR-101 in HUVECs *[40, 45, 46]*. We measured by Western Blot also the levels of H3K27m3, normalising to the levels of histone H3, and we found that even the epigenetic mark were lower in the GDM-HUVECs compared to the controls ($P<0.05$) according to the EZH2 levels (**Fig. 11f**).

We have examined changes of the other axis components. To investigate the autocrine signalling, specifically of the two growth factors responsible for axis activation, we cultured both groups of cells in serum starved condition for 24 hours (as specified in the methods), then we collected the conditioned medium (CM) and we analysed by ELISA the levels of FGF2 and VEGF. As shown in the figure **Fig. 13a, b**, we found lower FGF2 concentration in CM-GDM HUVECs compare with the CM from controls ($P<0.05$), while just a tendency toward lower VEGF concentration in CM from GDM HUVECs.

The graphs in the figure (**Fig. 14a, b**) represent the VEGF and KDM2B mRNA levels, measured in the HUVECs extracted from healthy and gestational diabetic mothers. Their levels tend towards a decreased in the

GDM lineages compare to the control, but without statistical difference. Coherently with the axis, and with other studies in which is shown the EZH2 transcriptional activation directly mediated by VEGF in endothelial cells, through the transcription factor E2F *[61],* we have found a positive Pearson's correlation between VEGF and EZH2 mRNA levels (Pearson r = 0.7 ; P<0.0005) (**Fig. 14c**).

Again, in accordance with the axis, we found positive correlation between EZH2 and KDM2B (Pearson r = 0.71; P<0.0005) and negative Pearson's correlation between miR-101 levels and KDM2B (Pearson r = - 0.63 ; P<0.005) (**Fig. 14d, e**).

3.4 Functional role of miR-101 in GDM HUVECs

To study the impact of miR-101 in GDM-HUVECs, cells were transfected with pre-miR-101, anti-miR-101, scramble control or non-transfected. **Fig. 15a** shows miR-101 changes in response to successful transfection. Moreover, EZH2 mRNA (**Fig. 15b**) and protein (**Fig. 16**) levels changed accordingly. The epigenetic mark H3K27me3 catalysed by EZH2 was decreased in GDM-HUVECs after pre-miR-101 transfection, in line with the EZH2 expressional changes (**Fig.16**); on the other side we found just a trend toward an increased H3K27m3 levels after anti-miR-101 transfection compared to the scramble control.

Next, we assessed the functional role of miR-101 in GDM-HUVECs (using healthy HUVECs for reference). Pre-miR-101 transfection reduced cell vitality (Trypan blue exclusion assay – **Fig. 17a**), while anti-miR-101

reduced apoptosis (**Fig. 17b**) of GDM-HUVECs. Importantly, the GDM-HUVEC capillary-like tube formation capacity on Matrigel was improved to the level of healthy HUVECs by anti-miR-101 (**Fig. 17c**). By contrast, changes in miR-101 expression did not influences the capacity of GDM-HUVEC to proliferate (BrdU incorporation data not shown) and only pre-miR-101 induced altered migratory capacity in GDM-HUVECs, while anti-miR-101 elicited not effect (**Fig. 18**).

In the light of the results we may conclude that the higher miR-101 levels and the decreased EZH2 levels found in GDM-HUVECs, can partially explain their impaired *in vitro* phenotypic properties compare with the controls. In fact, anti-miR-101 GDM-transfected cells, accompanied by restored EZH2 levels, have improved the capillary-like tube formation capacity on Matrigel and reduced apoptosis, similarly to the HUVECs derived from 'healthy' mothers.

3.5 EZH2 knock down induces apoptosis *in vitro* in GDM-HUVECs

To understand the role of EZH2 knock down in GDM HUVECs, firstly we examined the EZH2 inhibition testing the siRNA-mediated knock down of EZH2 (EZH2-siRNA) compare with the siRNA-control (siRNA-Ctr). As shown in **Fig. 19**, 12.5nM of siRNA-EZH2 were able to inhibit EZH2 protein levels by about 90% compared to the siRNA-Ctr ($P<0.05$) and to reduce H3K27m3 by about 20% ($P<0.05$) in both GDM-HUVECs and control-HUVECs. Sure about the siRNA specificity, we analysed the effect of EZH2 knock down (EZH2 KD) compared to the siRNA-Ctr, on miR-101 expression

levels (**Fig. 20**), on apoptosis (**Fig. 21a**) and on angiogenic capacity *in vitro* (**Fig. 21b**). In the figure **Fig. 20**, it's shown that miR-101 increased in GDM-HUVECs due to EZH2 KD ($P<0.05$ vs siRNA-Ctr), in accordance with published study *[45]* and tends toward an increased in Ctr-HUVECs ($P=0.1$ vs siRNA-Ctr). Moreover, the miR-101 increased is accompanied by augmented apoptosis in EZH2-siRNA transfected GDM-HUVECs ($P<0.05$ vs siRNA-Ctr) as expected (**Fig. 21a**).

Surprisingly, the GDM-HUVECs *in vitro* angiogenic capacity, already impaired by the previous hyperglycaemic environment, seems not be influenced by the EZH2 KD (**Fig. 21b**) differently from what we observed in the pre-miR-101 transfected cells (**Fig. 17c**). One possible explanation could be that, miR-101 levels reached with pre-miR-101 are much higher than the levels produced in EZH2 KD transfected cells, as shown the figure **Fig. 22**.

3.6 EZH2 knock down induces apoptosis in anti-miR-101 transfected GDM-HUVECs

We wanted evaluate also if the rescue observed with the anti-miR-101 can be annulled by the simultaneous down-regulation of EZH2. To answer that question, we performed the co-transfection with EZH2-siRNA/anti-miR-101, siRNA-Ctr/anti-miR-101, or siRNA-Ctr/scramble in GDM-HUVECs.

In response to the transfection, EZH2 mRNA levels increased with siRNA-Ctr/anti-miR-101 and decreased with siRNA-EZH2/anti-miR-101 compared to the control (**Fig. 23a**). Again, as expected miR-101 decreased in siRNA-Ctr/anti-miR-101 transfected cells compared to the control (**Fig. 23b**) and

that is accompanied by decreased apoptosis (P<0.05 vs siRNA-Ctr/scramble) and improved capillary network on Matrigel (P<0.05 vs siRNA-Ctr/scramble) (**Fig. 24a&b**). As previously mentioned, because EZH2 KD leads to increased miR-101 levels, we found no change in miR-101 levels between siRNA-Ctr/scramble and EZH2-siRNA/anti-miR-101 transfected cells. Moreover, the functional assays showed increased apoptosis in EZH2-siRNA/antimiR-101 transfected cells compared to siRNA-Ctr/anti-miR-101 and to siRNA-Ctr/scramble (**Fig. 24a**) and no changed in the capillary-like tube formation on Matrigel (**Fig. 24b**). In conclusion, EZH2 KD in anti-miR-101 transfected GDM-HUVECs increased apoptosis, while has no effect on angiogenic capacity *in vitro* compare with the only anti-miR-101 transfected cells, probably due to the contribute of other miR-101 targets involved in pathways controlling angiogenesis.

3.7 Analysis of EZH2 occupancy at miR-101 locus by chromatin immunoprecipitation (ChIP)

We hypothesized that EZH2 is required for the repression of miR-101 and that the lower EZH2 levels found in GDM-HUVECs may be responsible of the higher miR-101 levels. In fact other study demonstrated that the complex KDM2B/EZH2 binds miR-101 locus causing its repression on the transcriptional levels *[45].* We demonstrated that EZH2 KD caused miR-101 increase in GDM-HUVECs (**Fig. 20**), and a tendency toward higher miR-101 levels in EZH2-siRNA GDM-HUVECs than the EZH2 KD Ctr-HUVECs (P<0.1). We aimed demonstrate that EZH2 occupancy at the promoter

region of *miR-101 locus* is poorer in the GDM lineages compare with the controls, leading higher accessibility to transcription factors and promoting its transcription. To answer that, we performed ChIP experiment on the miR-101 promoter. In the **Fig. 25a** are showed the chromosome location of miR-101 locus and the recognized sequences of the primers used for the chromatin immunoprecipitation. We observed no significant difference between 'healthy' and GDM-HUVECs in the EZH2 occupancy on regulatory sequences of *miR-101 locus*, but a trend toward lower levels in the GDM-HUVECs compared to the controls (**Fig. 25b**).

3.8 MiR-101 increases after long exposure to high D-glucose in treated HUVECs (from healthy mothers)

It has been already widely shown that hyperglyceamia inhibits EC migration *in vitro [62, 63]* and impairs angiogenesis *in vivo* and *in vitro [64, 65].* However, the effects are related to the time and the concentration of D-glucose, beside of others experimental conditions. In fact, short treatment and/or medium concentrations of D-Glucose, reportedly enhanced ECs function through different intracellular signalling pathway *[66].*

To study the functional and molecular effect of hyperglycaemia *in vitro*, we treated the HUVECs extracted from 'healthy' mothers, for 12-24-48 hours with high glucose, as specified in the methods. The **Fig. 26** summarise the impact of hyperglyceamia *in vitro* on capillary-like tube formation on Matrigel. In the first 12 hours, 25mM and 12.5mM D-glucose (respectively indicated with HHD-Glu and HD-Glu) did not influence the HUVECs

angiogenic capacity; an increased angiogenesis response was observed after 24h in 12.5mM of D-glucose (HD-glu) ($P<0.05$ vs normal condition–N-). A longer exposure to hyperglycaemia *in vitro* impairs the angiogenic capacity: after 48 hours of treatment with 25mM of D-glucose (HHD-glu) the total length of tube decreased strongly compared to the controls. On the other side, the same concentration of 25mM of L-glucose (HHL-glu), and the 12.5mM of D- and L-glucose (HD-glu and HL-glu) have determined an improvement in the networking of tubes compare with the normal condition (N). The response to biologically inactive L-glucose observed is a result of increased osmolarity.

Then we checked in miR-101 levels and, as it's showed in the **Fig. 27**, after 24h of treatment with 25mM of D-glucose, miR-101 decreased and EZH2 (mRNA and levels) tends to a decreased (not statistically significant). But after 48 hours of treatment, with 25mM of D-glucose, miR-101 increased in 25mM D-glucose treated HUVECs ($P <0.05$ vs N), as in the analysed GDM cells. The model *in vitro* mimic the condition of hyperglyceamia in which are exposed the GDM extracted HUVECs *in utero* during the pregnancy, at least in the miR-101 up-regulation, in fact not significant differences has been found in EZH2 mRNA and protein levels (**Fig. 28a, b**).

3.9 MiR-101 increases after long exposure of D-glucose due to the diminished EZH2 occupancy at the promoter level

We performed the Chromatin Immunoprecipitation (ChIP) experiment on the miR-101 promoter region using antibody against EZH2 and H3K27m3,

as specified in the methods. Two set of primers have been used to amplify the putative EZH2 binding regions on miR-101 locus (**Fig. 25a**). The chromatin samples were obtained from one 'healthy' HUVECs lineage exposed for 48 hours to 25mM or 5mM of D-Glucose. That preliminary data, presented in the **Fig. 29**, shows that the occupancy of EZH2 on the *miR-101 locus* regulatory region is lesser in those HUVECs treated with high glucose compare with the normal control. That result is in accordance with the previous observance showing increased of miR-101 after long exposure of high D-glucose compared to the controls and, if confirmed with more experiments, could give an important explanation on how hyperglycaemia leads molecular and expressional alterations, influencing epigenetic regulator as EZH2 and its binding on the *miR-101 locus*.

3.10 The "glyceamic memory" studied *in vitro*

Having found the up-regulation of miR-101 *in vitro*, after 48 hours of treatment with high concentration of D-glucose, we wanted explore the persistence of that upregulation, after returned to normal glucose. We performed the "glyceamic memory" experiment culturing 'healthy' HUVECs with 25mM of D-Glucose for 48h, then in normal D-glucose for 5, 10 and 24 hours. Then we analysed miR-101 levels to explore if recovered cells return to normal miR-101 levels. The graph in **Fig. 30** shows that miR-101 tends to higher levels compared to the normal control, but without any statistical significance.

3.10 MiR-101 increases after long exposure to high D-Glucose due to the diminished EZH2 occupancy at the promoter level

'Healthy' HUVECs exposed for 48 hours to high or normal concentration of D-Glucose have been fixed, as specified in the methods, and prepared for the chromatin immunoprecipitation. As shown in the **Fig. 31**, the occupancy of EZH2 on the *miR-101 locus* regulatory region is lesser in those cells treated with high glucose compare with the normal control (N=1). That result is in line with the previous results: the miR-101 upregulation under high glucose condition *in vitro* and under chronic diabetic condition *in utero*. Moreover, it gives an important explanation how hyperglyceamia leads molecular/expressional alterations, influencing epigenetic regulator, as EZH2 and its binding on *miR-101 locus*, in turn promoting miR-101 transcription and the consequent EZH2 down-regulation.

3.11 Histological analysis of placental tissue from 'healthy' and GDM mothers

As specified in the methods, both GDM and 'healthy' placenta tissue has been collected and used for histological analysis (N=2).

The Hematoxylin-Eosin staining showed that the mesenchymal tissue of intermediate villi was denser and stained more intensely in GDM derived placenta than in normoglycemic women (**Fig. 32**). The mesenchyme normally has a loose arrangement, with numerous capillaries and is closely connected with the syncytiotrophoblast, while the placenta of women with GDM showed very dense mesenchyme, with fewer villous capillaries.

The Picrosirius Red staining revealed a greater condensation of collagen material organized around the vessels and villous stroma in placentas of women with gestational diabetes (**Fig. 32**). Our considerations are preliminary data needed confirmations because derived from just four placenta tissue (two controls and two gestational diabetic mothers).

4 DISCUSSION AND CONCLUSION

Epidemiologic studies suggest that intensive glyceamic control cannot reverse pre-established hyperglyceamia molecular and phenotypic alterations on endothelial cells. The involvement of epigenetic modifications and interconnected non-coding RNA-based mechanisms on 'glyceamic memory' reveal how heritable alterations, induced by transient hyperglyceamia, can persist and progress, even in normal glucose condition. That concept needs more detailed studies and, in this report we wanted contribute giving new experimental evidence in the field of gestational diabetes mellitus and its vascular complication.

In our study we firstly characterised the long-term effect of maternal gestational diabetes mellitus on the umbilical cord vein endothelial cells by functional assays *in vitro* and, not surprisingly, we observed impairment in endothelial cell phenotype in those cells derived from gestational diabetic mothers compared to the 'healthy' controls. Our findings were consistent with the hypothesized mechanisms where chronic hyperglyceamia can lead to long lasting endothelial dysfunction. In particular, we noticed that GDM-HUVECs showed reduced angiogenic capacity (analysed with Matrigel assay); lower proliferative index after stimulation with foetal bovine serum (FBS); impaired migration capacity (measured by scratch assays); and increased apoptosis, in comparison with HUVECs derived from 'healthy' controls. All functional assays were performed after five-six passages in culture in normal D-glucose (5mM); that reveal that the cells were still affected by the previous chronic hyperglyceamia *in utero*.

We aimed to investigate in microRNA deregulations and epigenetic modifications induced by the diabetic uterine environment on foetal umbilical vein endothelial cells. We started with miRs-screening of the miRs belonging to the miR-16 family *[56]*, which we already found upregulated in endothelial cells and other proangiogenic cells when diabetes mellitus was associated with critical limb ischemia *[57, 58].* In comparison with Ctr-HUVECs, the GDM-HUVECs showed a tendency toward higher levels of the miR-16 family, miR-503 especially, but without statistical significance.

Then we examine miR-101 levels and the other components of the FGF2-VEGF/KDM2B/EZH2-miR-101-EZH2 axis, never investigated before the field of diabetes and its vascular complications. The two growth factors FGF2 and VEGF are able to activate the axis and inhibit miR-101 promoting angiogenesis *[45].* In our report we showed lower FGF2 and a trend toward lower VEGF levels in conditioned medium from GDM derived-HUVECs compared to the 'healthy' controls.

Other reports have studied miR-101 in endothelial cells attributing an anti-angiogenic role, in part via inhibition of Enhancer of Zester Homolog 2 (EZH2) *[40].* We discovered higher miR-101 levels in the GDM-HUVECs compare with the controls ($P<0.05$) and a high positive Pearson's correlation between the miR-101 levels and the apoptosis (Pearson $r = 0.9$, $P<0.001$). Furthermore, increased miR-101 levels are accompanying with diminished levels of its target genes EZH2, both mRNA and protein, and reduced H3K27m3 global levels. In fact, H3K27m3 represents a covalent and thus lasting histone modification that can be removed by histone demethylases

[34]. EZH2 is essential for the H3K27m3 propagation and maintenance and its decrease or loss would lead to detectable reduction of H3K27m3 mark, as we found, with alteration in gene expression and endothelial function. A recent study, aimed to understand the role of EZH2 in the control of gene expression in endothelial cells, have identified 946 genes upregulated by >2-fold due to EZH2 knockdown, in accordance with its repressive function. Importantly, many of these genes are implicated in endothelial cell dysfunctions and cardiovascular disease *[42].*

We demonstrated that, the induced up-regulation *in vitro* of EZH2 by anti-miR-101 in the GDM cells decreased their levels of apoptosis and improved the angiogenic phenotype affected by hyperglyceamia in utero, restoring the endothelial tube formation on Matrigel as the control lineages. On the other side, the inhibition of EZH2 through pre-miR-101 transfection reduced cell vitality (Trypan blue exclusion assay), reduced the migration (scratch assay) and the angiogenic capacity (matrigel assay), capacities already compromised of the GDM-HUVECs.

In the light of our results, we wanted also deeper explore the effect of EZH2 knock down in GDM-HUVECs and especially in anti-miR-101 transfected GDM-HUVECs. We observed increased levels of miR-101 due to EZH2 KD ($P<0.05$), in accordance with published study *[45]* and augmented apoptosis. Surprisingly, the GDM-HUVECs *in vitro* angiogenic capacity, seems not be influenced by the EZH2 KD, differently from what we observed in the pre-miR-101 transfected cells. One possible explanation might be that the levels of miR-101 reached with pre-miR-101 are much higher than the miR-101

levels in EZH2 KD transfected GDM cells. That could make the difference because the alterations in miRs expressional levels may affect proportionally the cell phenotype, depending on the range of target gene interested. In fact, miR-101 can influence many other proteins, and directly/indirectly influence a variety of target genes, not just EZH2 *[67, 68, 69].*

We confirmed with an *in vitro* model of hyperglycaemia that high glucose significantly impaired the function of HUVECs, as shown in many reports, with the novelty of concomitantly upregulation of miR-101 after long exposure to D-Glucose (48h with 25mM of D-Glucose, compared to the normoglycemic and osmotic controls). Importantly, the ChIP on the miR-101 locus permitted to detect the occupancy of EZH2 on regulatory region and to discover that is lesser in those HUVECs treated with high glucose compare with the normal control ($P<0.05$). That result explain how hyperglycaemia leads molecular and expressional alterations, influencing epigenetic regulator as EZH2 and its binding on the miR-101 locus, in turn, promoting miR-101 transcription and its consequent up-regulation. Higher miR-101 may stabilise the EZH2 down-regulation, influencing gene expression and the endothelial cell phenotype.

Our study is in line with the 'glyceamic memory' theory, where chronic hyperglycaemic conditions lead persistent outcomes, through epigenetic changes and alterations in miRs levels. That finding can also contribute to the knowledge about the molecular pathways activated by hyperglycaemia

in utero on the foetal endothelial cells, opening ways to new targets and novel future therapeutic interventions.

The histological analysis of the placenta tissue demonstrated that the mesenchyme of the placenta from GDM women is denser than the normal placenta due to the accumulation in collagen material. Our analysis confirmed previous studies in which hyperglyceamia has been associated with higher production of collagen by the vascular endothelium *[55]* and also intensified deposition of the extracellular vascular amyloid, which consists on a heterogeneous mix of fibrillar proteins *[53, 54].* The production of these proteins may explain the appearance of more condensed mesenchyme around blood vessels.

5 FIGURES

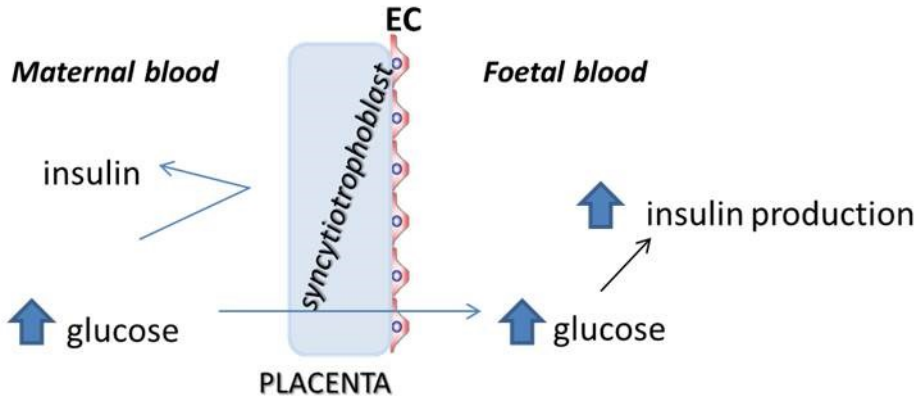

Fig. 1

The "Pedersen's hyperglycaemia-hyperinsulinemia hypothesis"

In diabetic condition, the high amount of maternal D-glucose can cross the placental barrier becoming available to the foetus, establishing chronic foetal hyperglyceamia. The maternal insulin does not cross the placenta and the developing foetal pancreas responds to a D-glucose load by increasing synthesis and release of insulin, which acts as a foetal growth hormone. This is the basic concept of the "Pedersen's hyperglycaemia-hyperinsulinism hypothesis", where foetal overgrowth due to hyperinsulinemia is the response to increased transplacental D-glucose transfer.

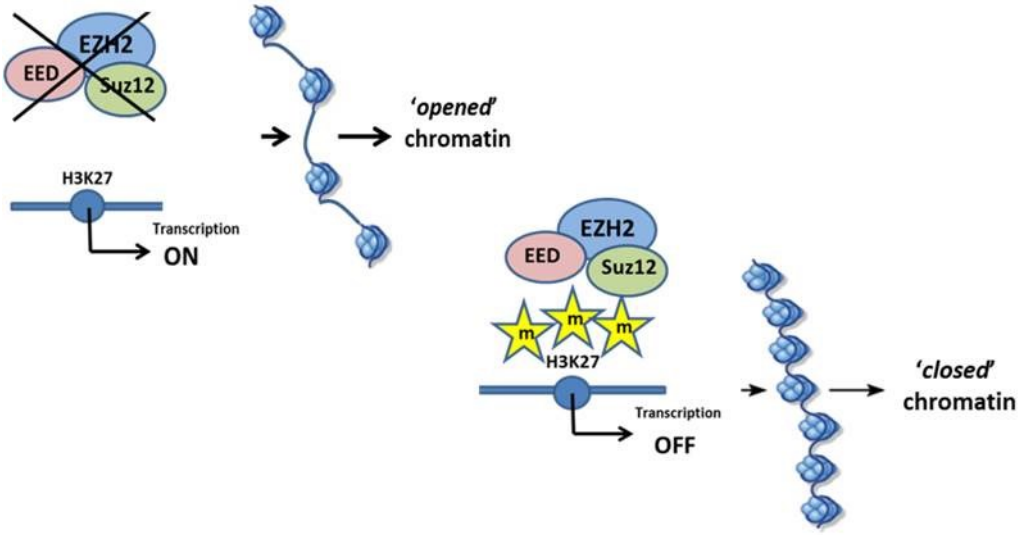

Fig.2

Role of Enhancer of Zester Homolog2 (EZH2)

The protein Enhancer of Zester Homolog2 (EZH2) is a well-characterized regulator of the epigenome. It's the only protein of the Policomb Repressor Complex2 (PRC2) with a histone methyltransferase activity that initiates and maintains the methylation of Lys27 (H3K27) on histone H3.

According to the 'histone code' hypothesis, histone marks are deposited by 'writer' proteins and recognized by 'reader' proteins. EZH2, together with PRC2 and with chromatin regulators trigger the transition between open (permissive) to close (non-permissive) chromatin, regulating gene transcription. In fact, the epigenetic mark H3K27m3 mediates the long term epigenetic gene silencing.

List of principal microRNAs involved in endothelial cells function:

miRNA	Target gene	ECs functional effect	Reference
miR-320	VEGF, FGF, IGF	(-) proliferation, migration, angiogenesis	Wang et al
miR-503	CDC, CCNE1	(-) proliferation, migration, angiogenesis	Caporali et al
miR-221/-222	Ckit, p27kip1, p57kip2	(-) proliferation, migration, angiogenesis, (+) apoptosis	Togliatto et al
miR-126	VCAMI, SDF1, PAK1	(-) inflammation, (+) angiogenesis	Wang et al
miR-210	Ephrin A3	(+) angiogenesis	Fasanaro et al
miR-101	EZH2	(-) angiogenesis	Smits et al

Table I

Principal miRNAs involved in ECs function.

Table showing some of the principal microRNAs involved in proliferation, migration, and angiogenesis.

	Control lineages	GDM lineages	
	N=24	N=22	p-value
age (years)	31.12 ± 6.54	35.13 ± 7.41	0,1
smokers (N)	1	1	
weight (Kg)	77.00 ± 15.48	73.73 ± 14.74	0,5
obese (N)	3	4	
epidural delivery (N)	3	6	
pregnancy at risk (N)	0	1	

Table II

Characteristics of the healthy mothers and gestational diabetes mellitus (GDM) mothers

The table shows the characteristics of the 'healthy' (N=24) and gestational diabetic (N=22) mothers, donors of the umbilical cords from which have been extracted the HUVECs for the study.

Quantitative data are expressed as mean and standard deviation (SD).

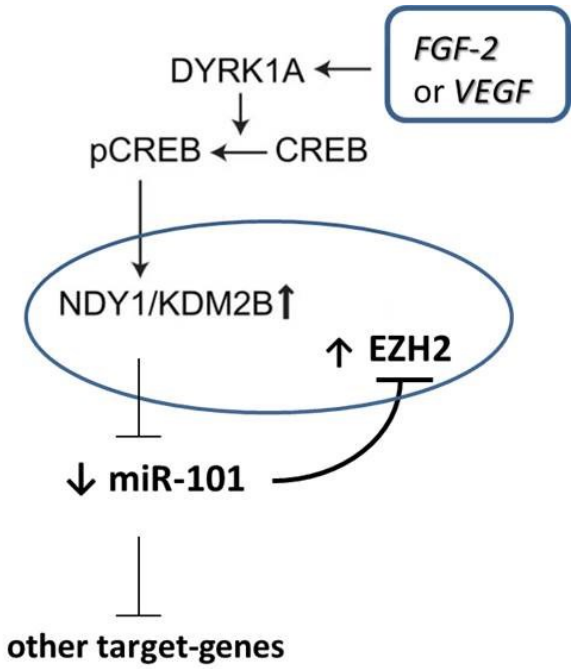

Fig. 3

FGF2 or VEGF-KDM2B/EZH2-miR-101-EZH2 axis

FGF2 and VEGF regulate cell proliferation, migration and angiogenesis, in part through the phosphorylation of CREB, the consequent NDY/KDM2B upregulation and the recruitment of basally expressed EZH2. The complex NDY/KDM2B/EZH2 acts in several regulatory sequences leading gene repression. In particular, it binds and represses the miR-101 locus increasing the target gene EZH2 and stabilizing the miR-101 initiated repression.

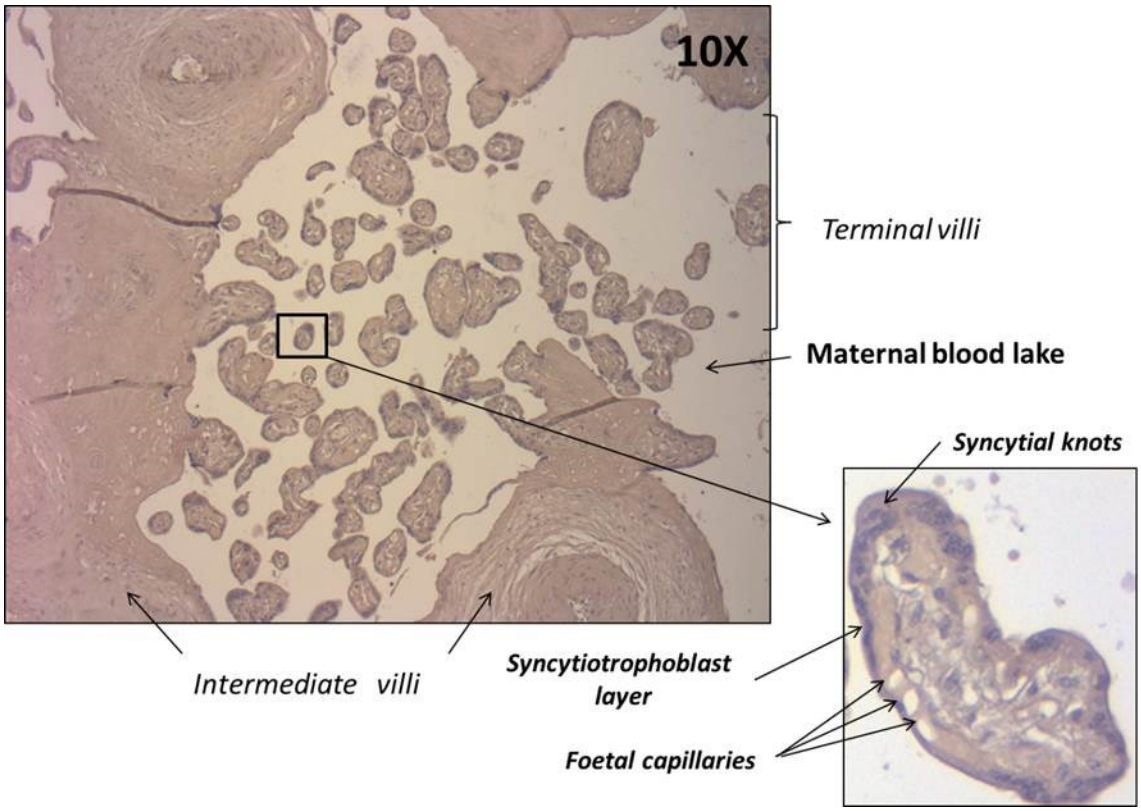

Fig.4

Histological analysis of placenta

The chorionic villi gradually branched into intermediate and terminal villi, which are surrounded by a syncytiotrophoblast layer and syncytial knots, formed by group of nuclei. The maternal blood circulates in the intervillous space, while the foetal blood is separated from maternal blood by the placental membrane. The centre of the villi contained loose mesenchymal tissue with fibroblasts, macrophages and blood vessels. The structure and size of vessels into the villi is proportional to the thickness, small villi contained only capillaries (foetal capillaries).

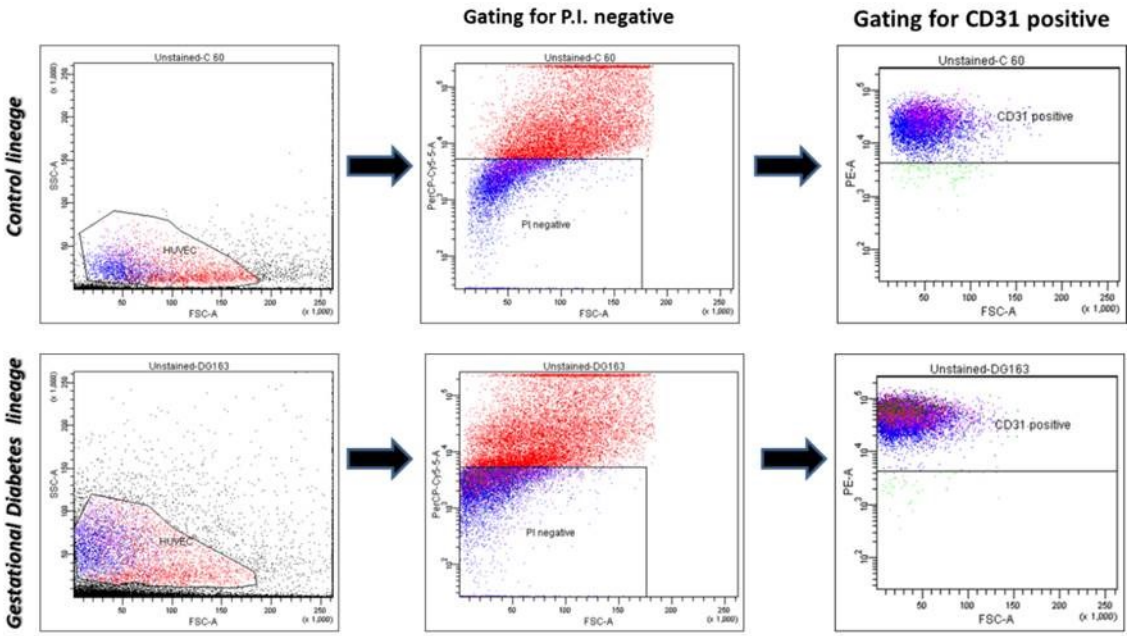

Fig. 5

Flow cytometry for endothelial marker (CD31-positive/PI negative) in 'healthy' controls and GDM lineages

The purity of the cells has been investigated by FACS using the endothelial marker CD-31. As the figure shows, both GDM-HUVECs and Ctr-HUVECs are CD-31 positive (≥95%).

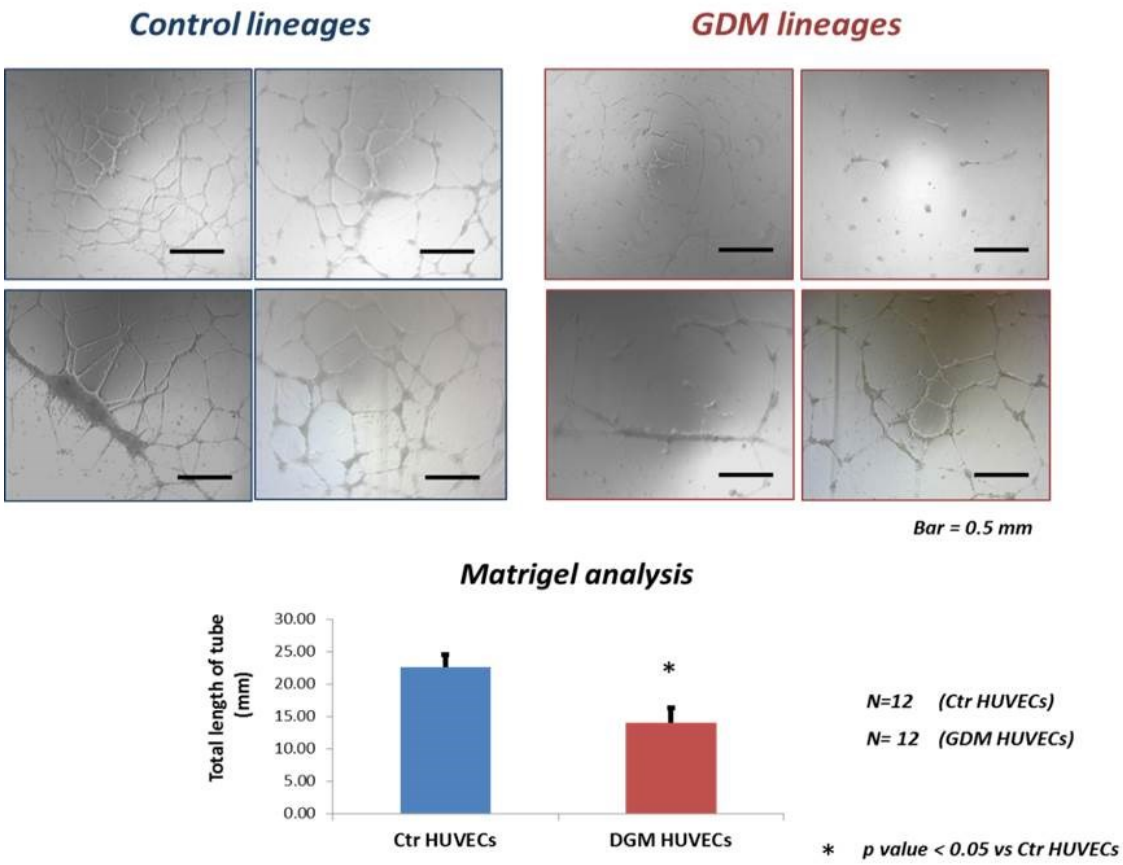

Fig. 6

Analysis of capillary-like tube formation on Matrigel

The HUVECs extracted from gestational diabetes mellitus (DGM) mothers have lower angiogenic capacity, measured analysing the network formed on Matrigel, compared to the control group of HUVECs. Data are presented as mean SEM. The data are obtained from a triplicate of n=12 (Control lineages or GDM lineages). * p value < 0.05, as compared with control group.

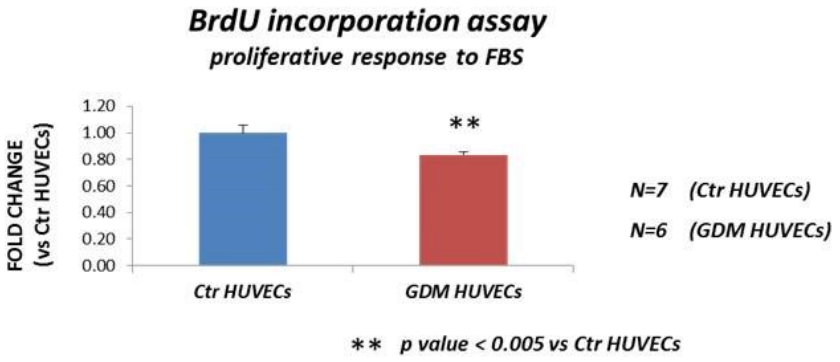

Fig. 7

BrdU incorporation assay in response to FBS

The HUVECs extracted from gestational diabetes mellitus (DGM) mothers have lower proliferative capacity in response to FBS. Briefly, both lineages were cultured for 1 hour in strong serum starved condition (EGM2 without FBS), then for 24 hours in EGM2 (0.5% FBS) or in normal condition. Proliferative index has been calculated by the ratio between the BrDu incorporation values in starved condition and in normal condition, for each lineage. The data are obtained from n=7 Controls and n=6 GDM-HUVECs. Data are presented as mean SEM. ** p value < 0.005, as compared with control group.

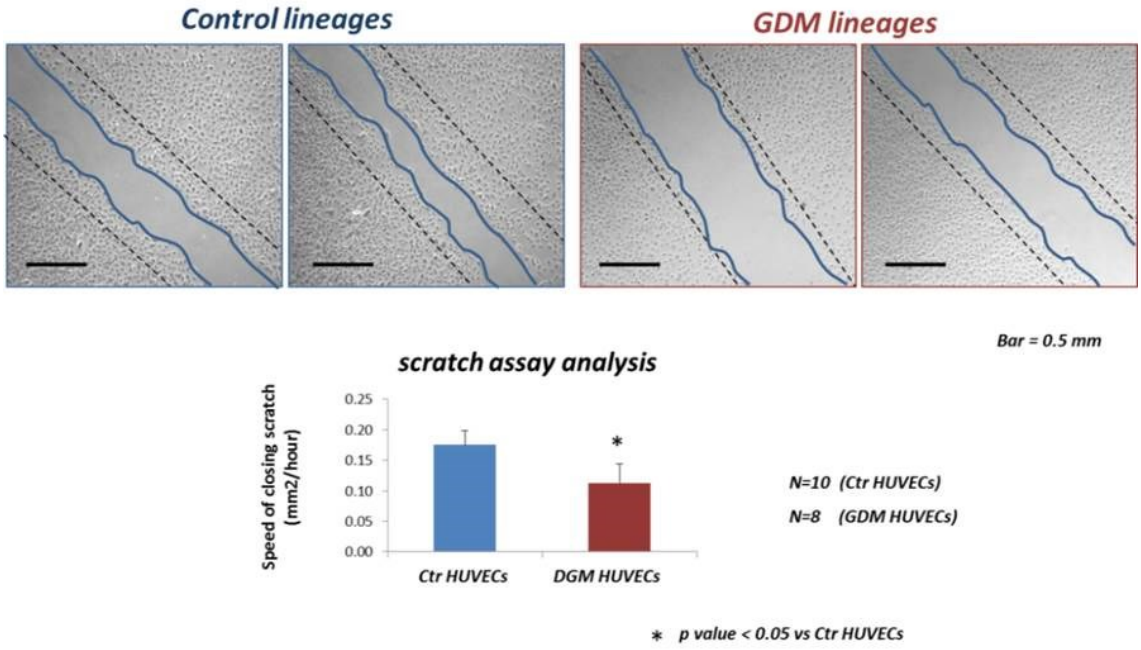

Fig. 8

Analysis of hound healing in vitro by scratch assay

The HUVECs extracted from gestational diabetes mellitus (DGM) mothers have lower capacity of closing scratch compared the control group of HUVECs extracted from healthy mothers. Data are presented in mm2/hour, as mean SEM. The data are obtained from n=10 Controls and n=8 GDM lineages. * p value < 0.05, as compared with control group.

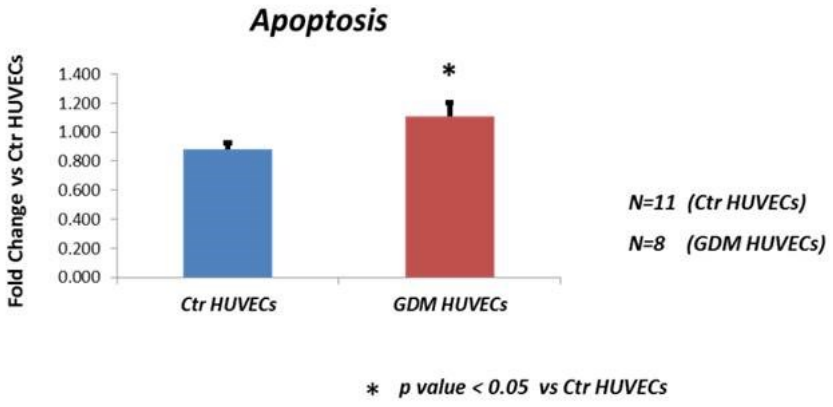

Fig. 9

The results of the levels of apoptosis of measured with the ELISA kit

The graph shows an increase of apoptosis in the gestational diabetic mellitus (DGM) mothers extracted lineages compare the controls. Data are presented as mean SEM. The data are obtained from n=11 Control HUVECs and from n=8 GDM-HUVECs.

* p value < 0.05, as compared with control group.

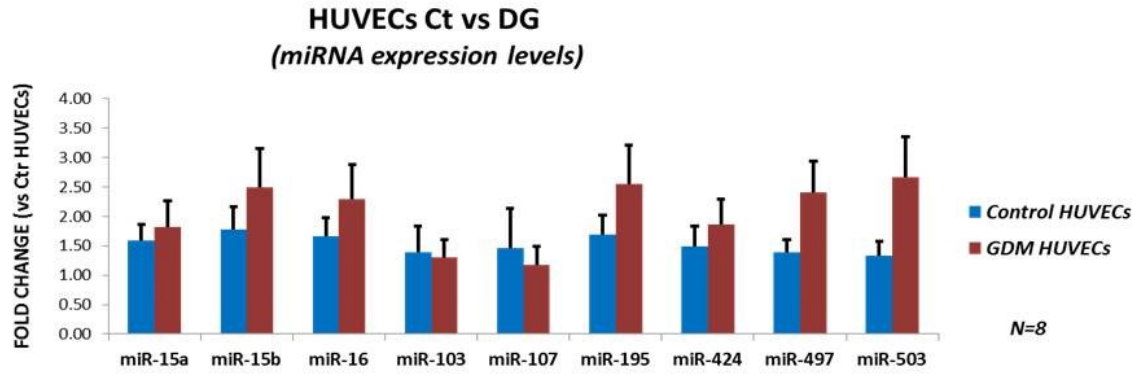

	miR-15a	miR-15b	miR-16	miR-103	miR-107	miR-195	miR-424	miR-497	miR-503
Control HUVECs	1.59	1.77	1.66	1.38	1.45	1.69	1.49	1.38	1.33
GDM HUVECs	1.81	2.49	2.29	1.30	1.18	2.55	1.86	2.41	2.66
SEM	0.275	0.397	0.315	0.447	0.681	0.332	0.338	0.218	0.250
	0.455	0.658	0.594	0.297	0.315	0.659	0.427	0.529	0.680
T.Test	*0.68*	*0.36*	*0.36*	*0.89*	*0.72*	*0.26*	*0.50*	*0.09*	*0.08*

Fig. 10

MicroRNAs screening for miR-16 family

HUVECs from 'healthy' and from GDM mothers (N=8) has been screened for the microRNAs belonging to the extended miR-16 family (miR-15a, miR-15b, miR-16, miR-103, miR-107, miR-195, miR-424 and miR-497, miR-503) already found upregulated in endothelial cells and other proangiogenic cells in the field of diabetes mellitus associated with critical limb ischemia. We found a trend towards increased levels in GDH HUVECs compare with the 'healthy' lineages, but without statistical significance.

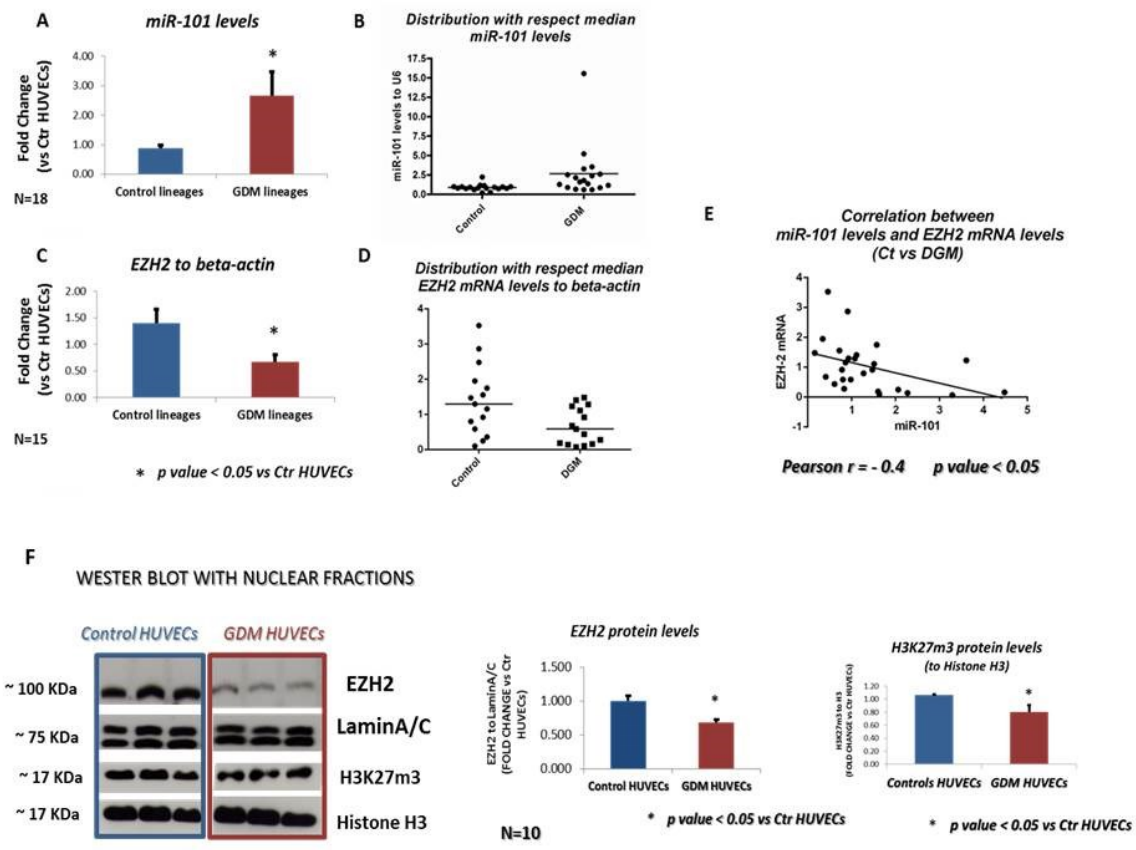

Fig. 11

The miR-101 levels and EZH2 (mRNA and protein) levels evaluated in gestational diabetic and healthy HUVECs lineages

The levels of miR-101 (a) and EZH2 mRNA (c) analysed in GDM and control HUVECs, with the respective distribution with respect median (b&d). Their values are negative correlated (Pearson r =-0.4, p value < 0.05), as is showed in the graph of the Linear Regression (e). miR-101 levels are higher in the GDM-HUVECs compared to the controls, while EZH2 mRNA and protein levels (f), measured by Western blot normalising with LaminA/C, are lower respect to the controls. Coherently with EZH2 levels, even the epigenetic

mark H3K27m3 normalised to Histone H3, is lower in the GDM lineages compare with the controls. All RT-PCR data are presented as mean SEM.

* p value <0.05, as compared with control group.

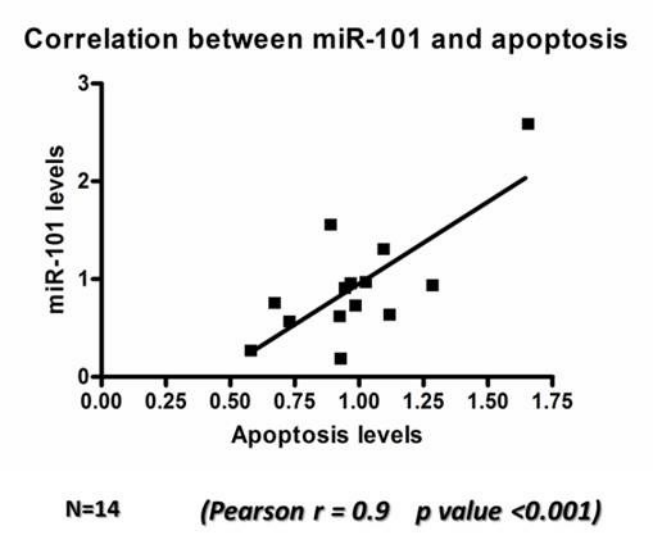

Fig. 12

Positive Pearson's Correlation between miR-101 levels and apoptosis

HUVECs from 'healthy' and GDM mothers has been analysed in their miR-101 levels and apoptosis. The graph shows that their levels are highly positively correlated, the Pearson's Coefficient is 0.9 (P<0.001).

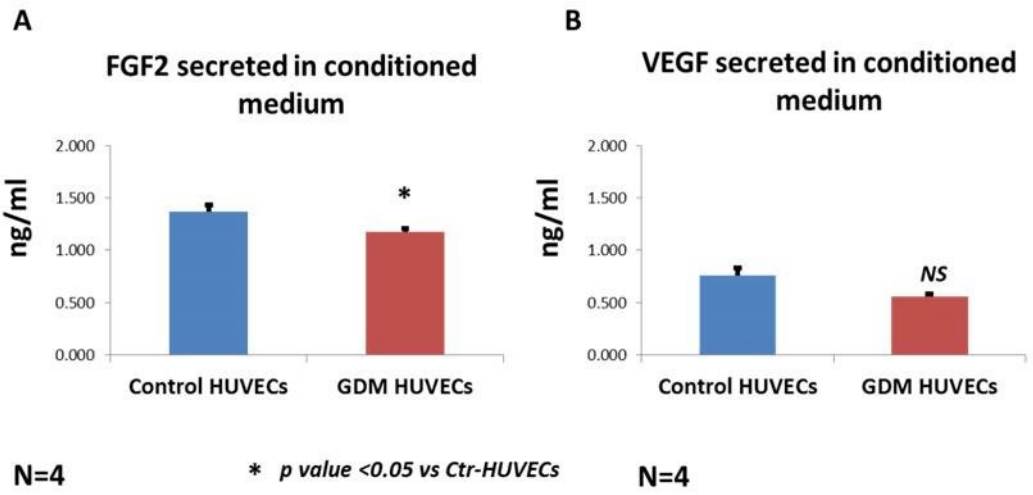

Fig. 13

FGF2 and VEGF secreted levels evaluated in gestational diabetic and healthy HUVECs

GDM-extracted HUVECs and healthy lineages were cultured in serum starved condition for 24hours (as specified in the methods). We collected the conditioned medium, and then we measured the levels of FGF2 (a) and VEGF (b) by ELISA. GDM HUVECs secreted lower FGF2 compared to the control lineages ($P<0.05$), while the difference found in VEGF levels is not significant ($P=0.1$).

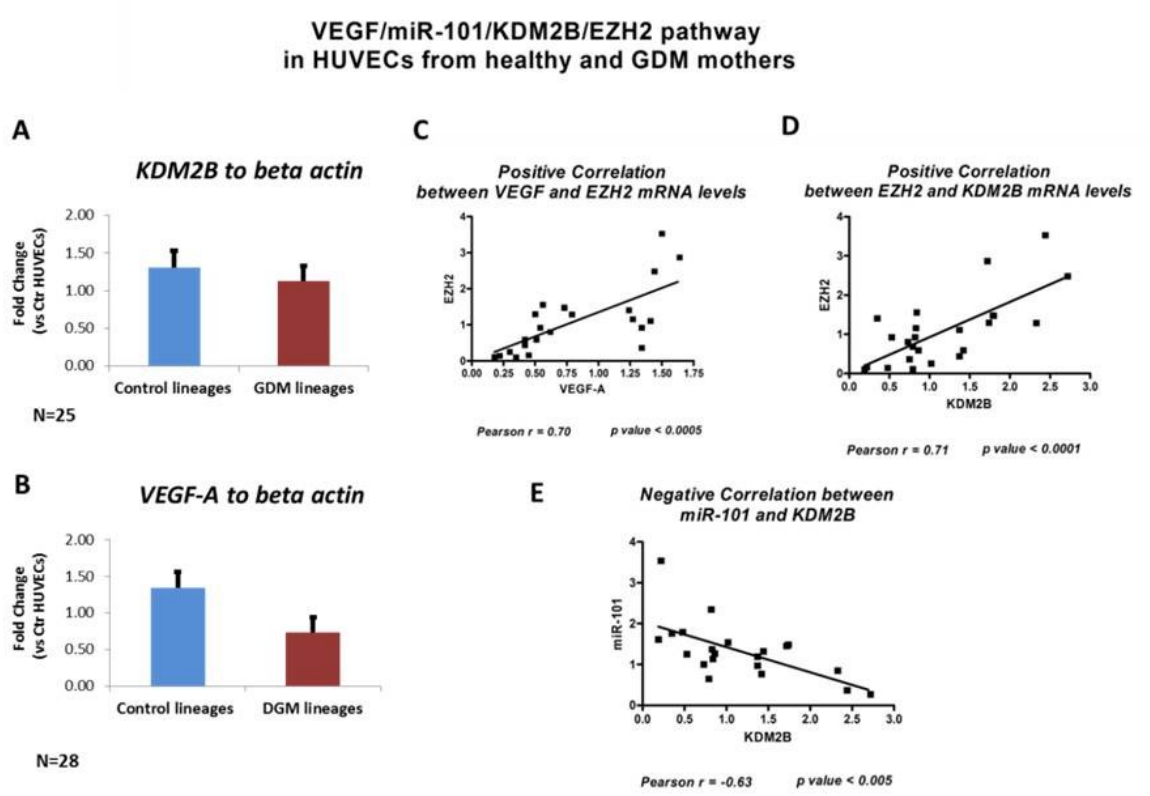

Fig. 14

The components of the VEGF-A/KDM2B/miR-101/EZH2 axis measured on the HUVECs extracted from healthy and gestational diabetic mothers.

The mRNA levels of KDM2B (a) and VEGF (b) measured in gestational diabetic extracted HUVECs tend to lower levels compare with the control lineages, but there is no a significant difference. The mRNA levels of VEGF are correlated positively with the EZH2 mRNA levels according to the axis (c); again EZH2 and KDM2B are positively correlated (d), conversely KDM2B mRNA values are negative correlated with the levels of miR-101 (e).

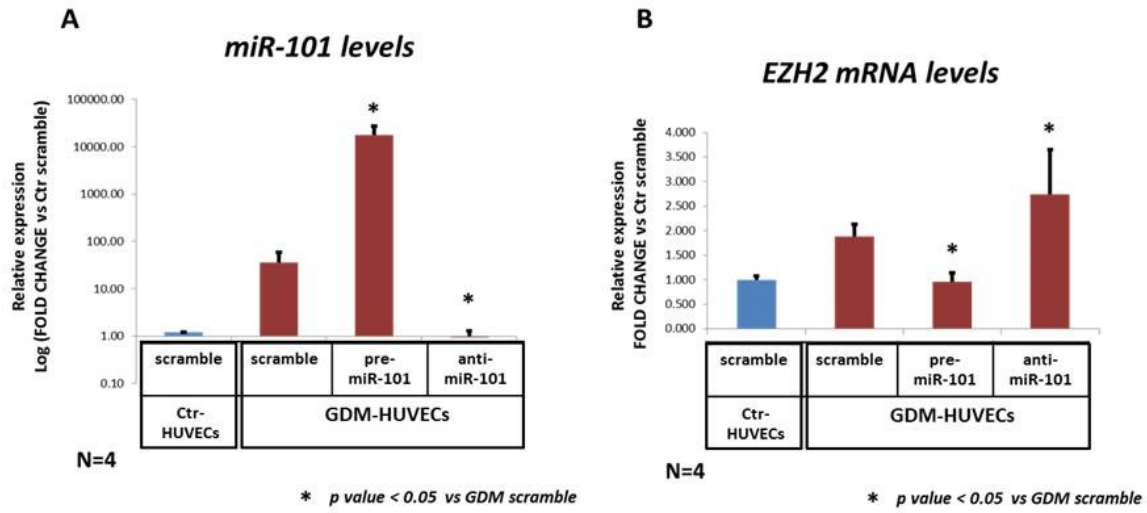

Fig. 15

Relative expression of miR-101 and EZH2 mRNA levels in pre-miR-101, anti-miR-101 or scramble transfected HUVECs

The two graphs represent the relative expression of miR-101 (a) and EZH2 mRNA (b) in Control HUVECs and GDM-HUVECs, both transfected with scramble, and GDM lineages also with pre-miR-101 and anti-miR-101. Data are presented as mean SEM. * p value <0.05, as compare with control group.

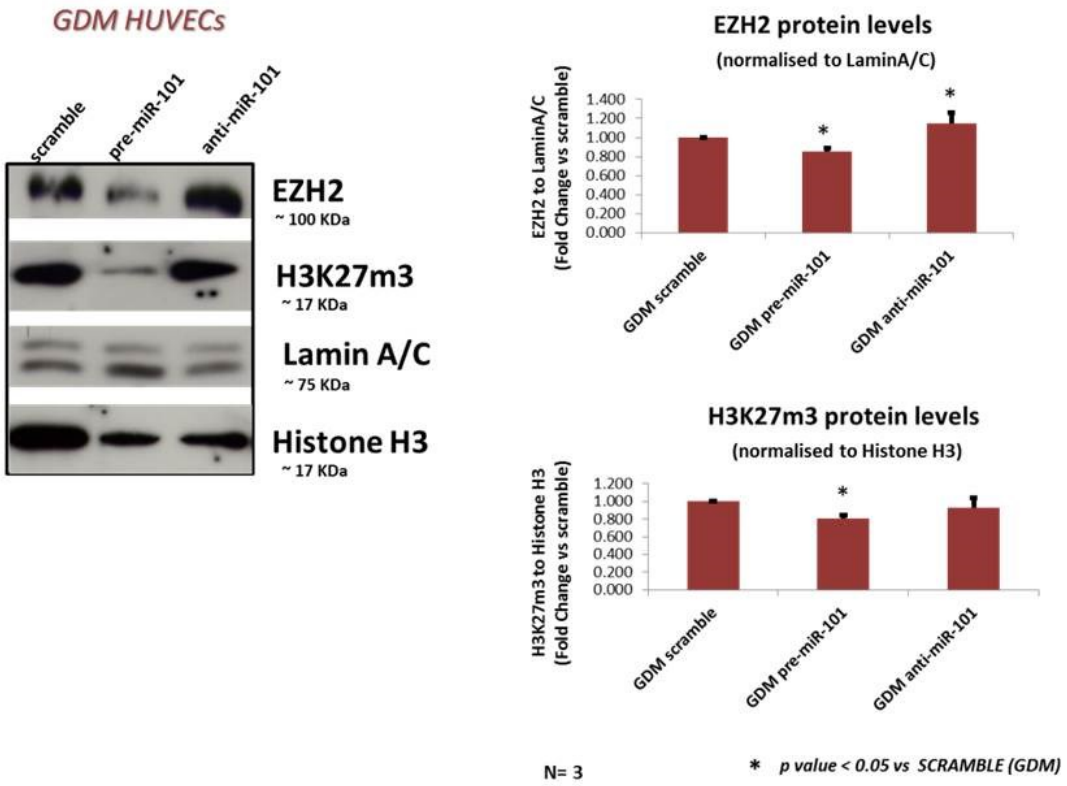

Fig. 16

EZH2 and H3K27m3 protein levels analysed by Western blot in pre-miR-101, anti-miR-101 or scramble transfected GDM HUVECs

The two graphs represent the protein levels of EZH2 and H3K27m3, respectively normalised to LaminA/C and Histone H3, in GDM-HUVECs transfected with scramble, pre-miR-101 and anti-miR-101. Data are presented as mean SEM. * p value <0.05, as compare with scramble (GDM) control.

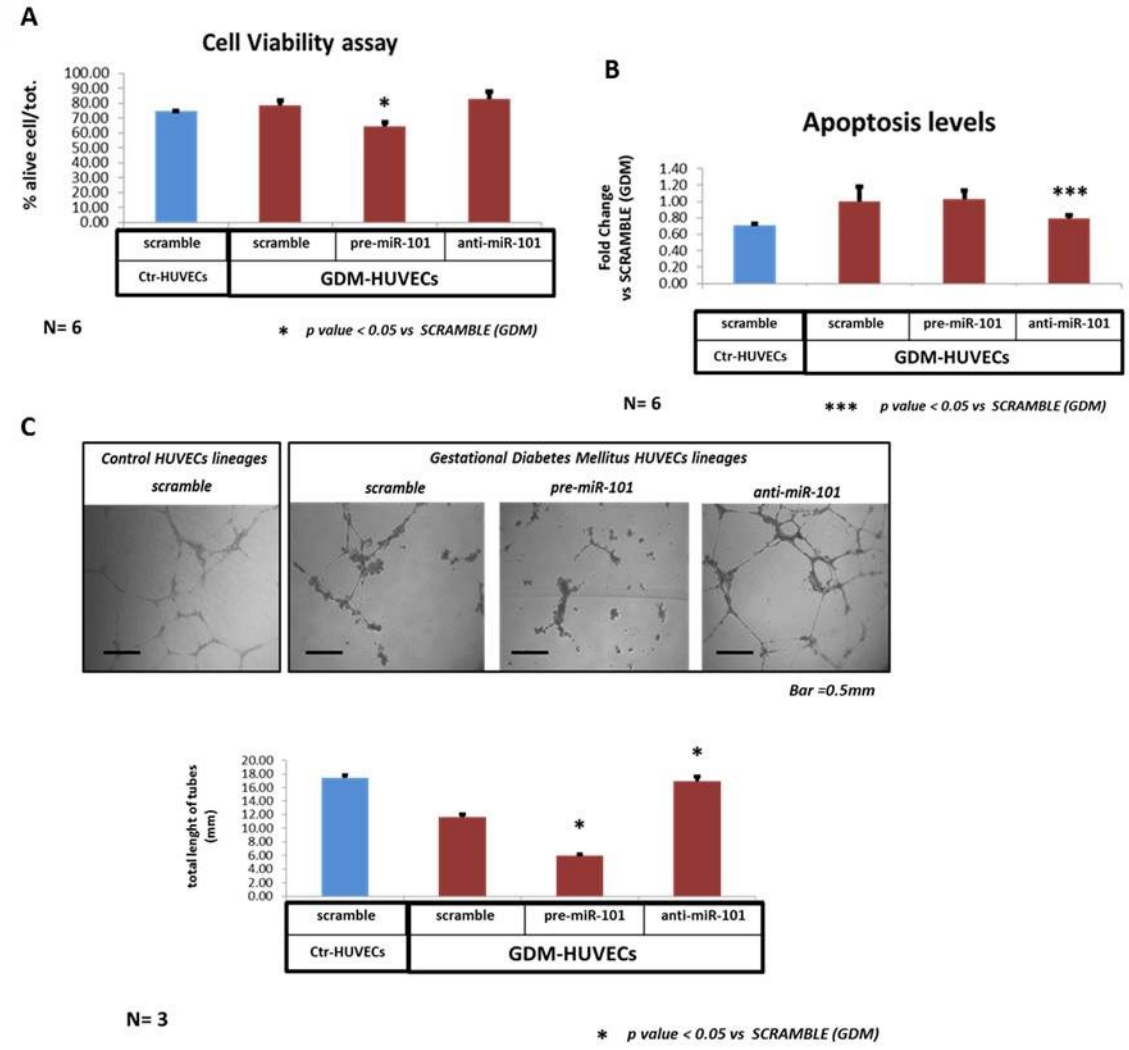

Fig. 17

Role of miR-101 in GDM lineages: in cell viability, in apoptosis and in capillary-like tube formation on Matrigel

GDM lineages were transfected with pre-miR-101, anti–miR-101, or scramble; also the control lineages transfected with scramble. (a) Then have been analysed the cell viability with Trypan Blue as % of alive cells/total cells; (b) the levels of apoptosis, calculated in fold change, normalizing to the average of the scramble (GDM lineages) values, as a control.

All data are expressed as mean SEM. * p value < 0.05 as compare with SCRAMBLE (GDM lineages), *** p value < 0.0005 as compare with SCRAMBLE (GDM lineages).

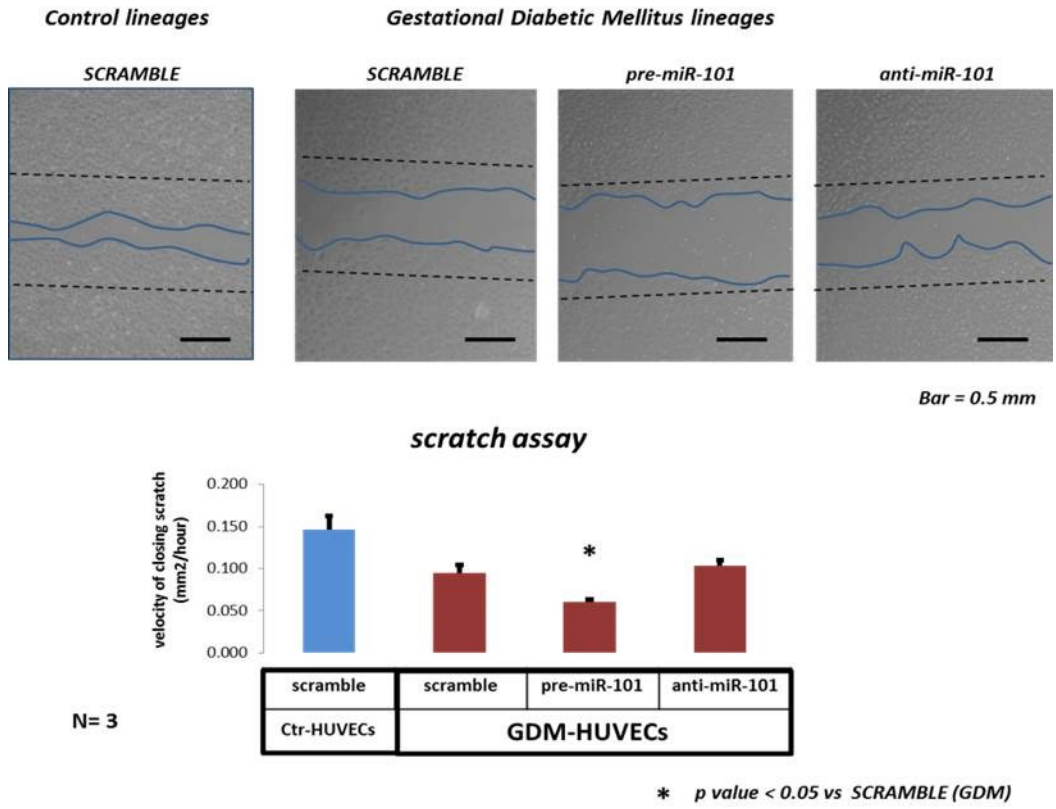

Fig. 18

Role of miR-101 in hound healing *in vitro* assay (scratch assay) in GDM lineages

GDM lineages (N=3) were transfected with pre-miR-101, anti–miR-101, or scramble; also the control lineages transfected with scramble. The induced miR-101 overexpression decreased the migrative capacity of the GDM-HUVECs compare with the scramble control. The migrated area of the

wound edge was quantified as mm2/hour. Scale bar = 0.5mm. Data are presented as mean SEM (n = 3).

* p value <0.05, as compared with scramble GDM-HUVECs group.

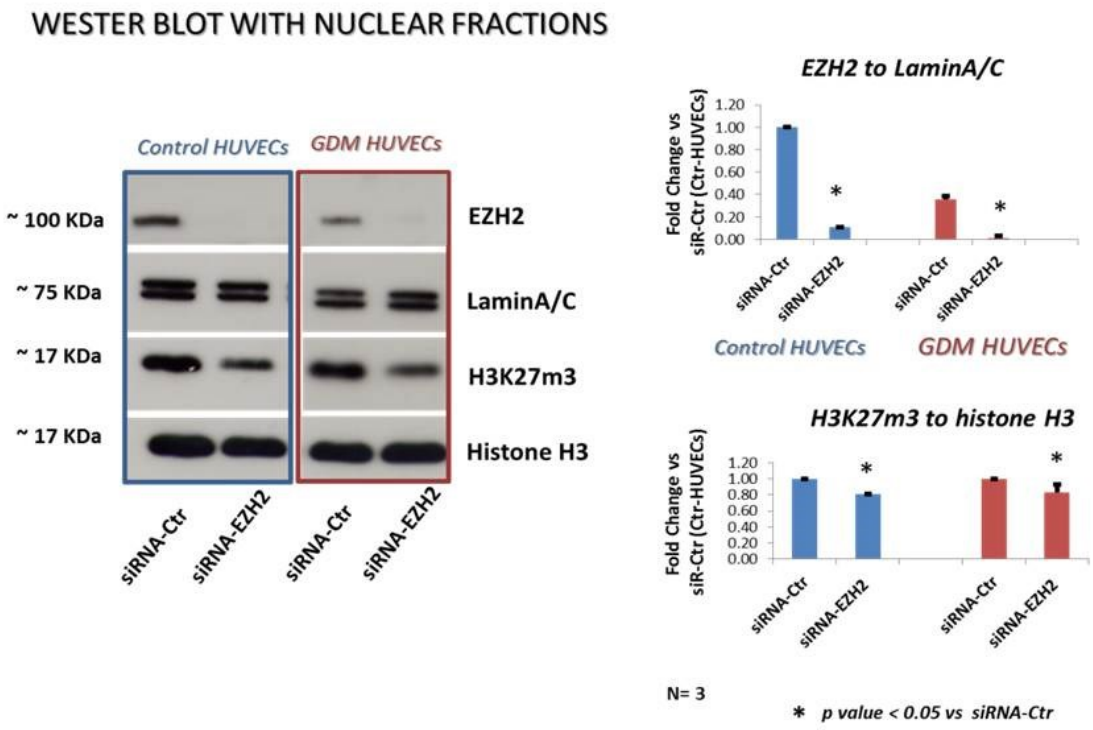

Fig. 19

EZH2-siRNA-mediated knock down in healthy and GDM lineages

HUVECs have been transfected with EZH2-siRNA and siRNA-Ctr, as specified in the methods. Then, nuclear fractions has been extracted and analysed by Western blot. EZH2 and H3K27m3 protein levels decreased in EZH2-siRNA transfected cells compare with the controls. Data are presented as mean SEM (n = 3).

* p value <0.05, as compared with siRNA-Ctr group.

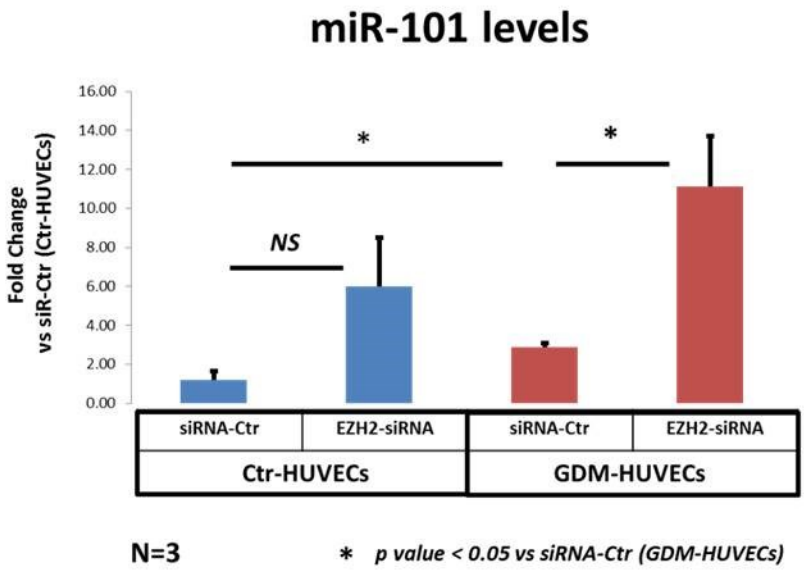

Fig. 20

EZH2 knock down leads the upregulation of miR-101 in EZH2-siRNA transfected GDM-HUVECs compared to the siRNA-Ctr

Control and GDM lineages (N=3) were transfected with EZH2-siRNA, or siRNA-Ctr . The graph shows the increased miR-101 levels after EZH2 KD in GDM-HUVECs ($P<0.05$ vs siRNA-Ctr). All data are expressed as mean SEM. * p value <0.05 as compare with siRNA-Ctr (GDM-HUVECs).

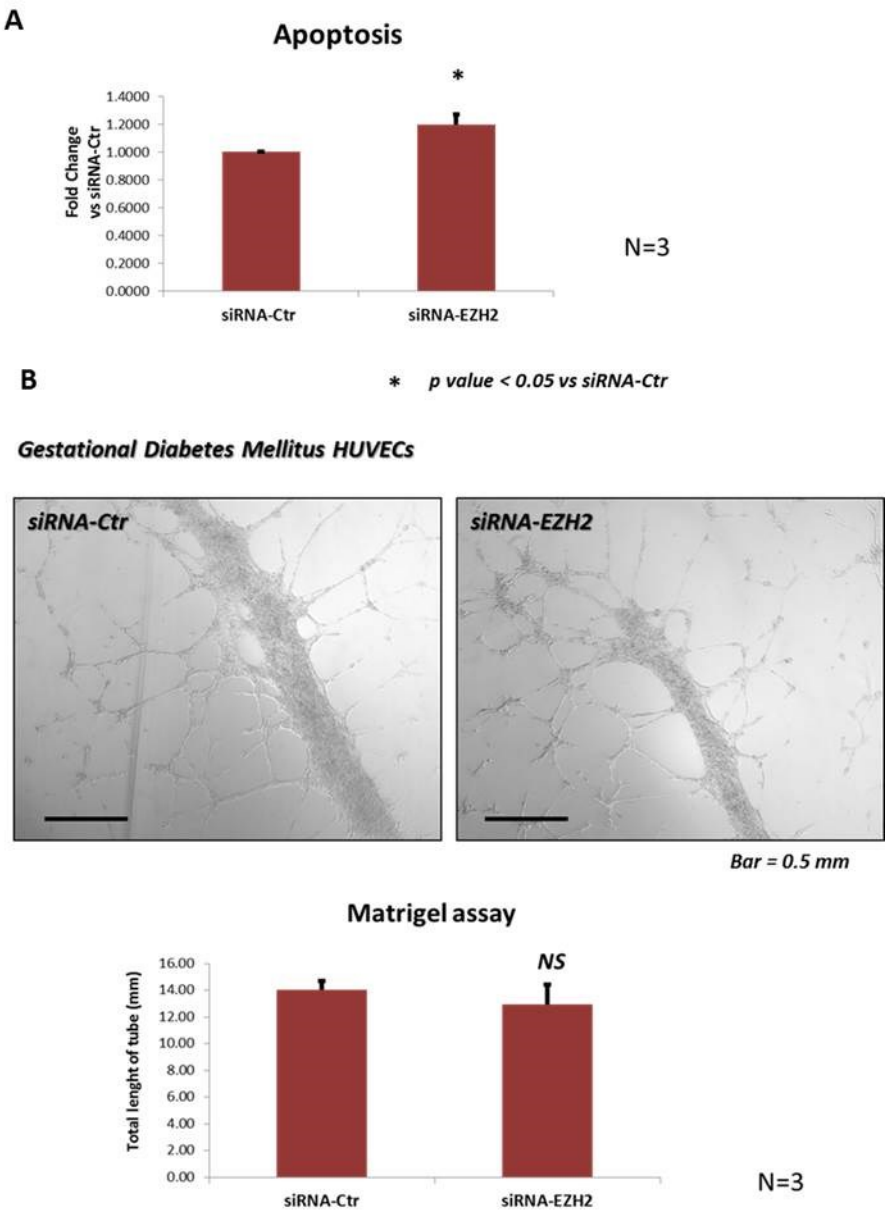

Fig. 21

EZH2 knock down in GDM-HUVECs increased apoptosis compared to the siRNA-Ctr, while doesn't affect significantly the network on Matrigel

GDM lineages (N=3) were transfected with EZH2-siRNA, or siRNA-Ctr then analysed in the levels of apoptosis and in angiogenic capacity *in vitro*.

(a) The apoptosis of the GDM extracted HUVECs increased in EZH2-siRNA compare with the siRNA-Ctr, (b) while the angiogenic capacity is not affected by the EZH2 KD. All data are expressed as mean SEM.

* p value < 0.05 as compare with siRNA-Ctr.

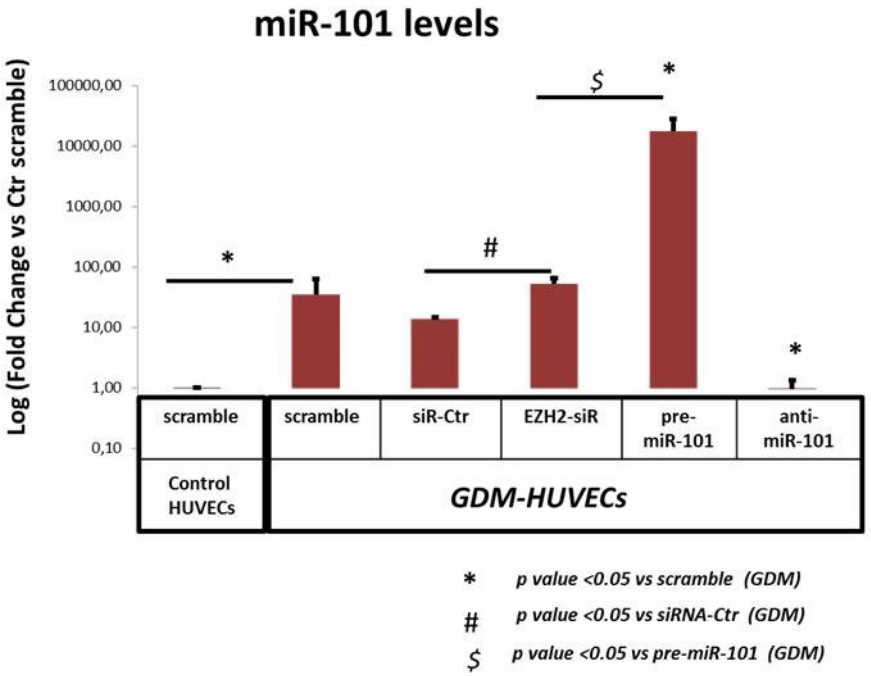

Fig. 22

Relative miR-101 quantification between GDM-HUVECs transfected with pre-miR-101, anti-miR-101, EZH2-siRNA, siRNA-Ctr, scramble, and 'healthy' HUVECs with the only scramble

GDM-HUVECs (N=3) were transfected with pre-miR-101, anti-miR-101, EZH2-siRNA, siRNA-Ctr, scramble while 'healthy' HUVECs transfected with the only scramble control, as a reference. Then, miR-101 levels have been measured. All data are expressed as mean SEM. * p value <0.05 as compare with scramble (GDM-HUVECs); # p value <0.05 as compare with

siRNA-Ctr (GDM-HUVECs); $ p value <0.05 as compare with pre-miR-101 (GDM-HUVECs).

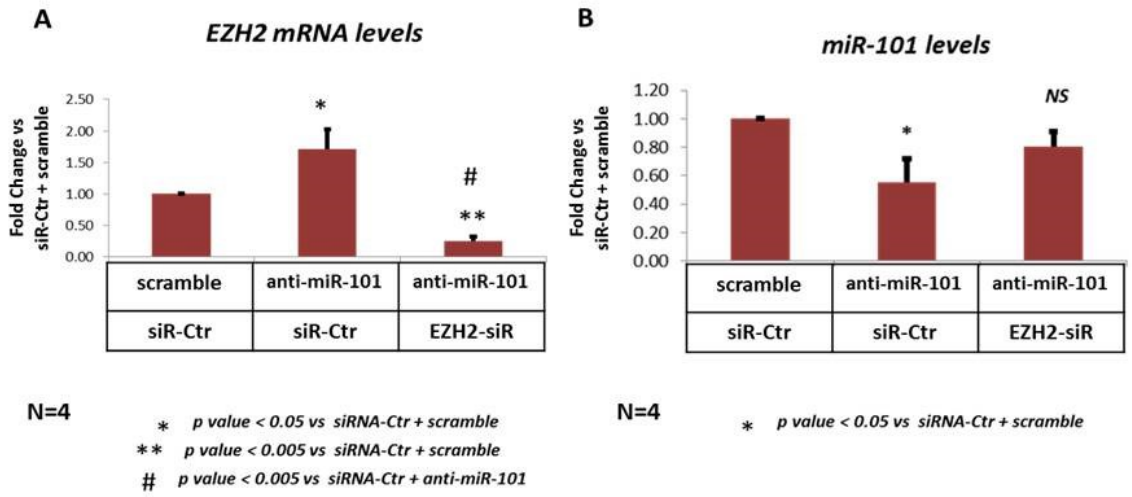

Fig. 23

EZH2 mRNA and miR-101 levels in co-transfected GDM-HUVECs

GDM-HUVECs (N=4) has been cotransfected with siRNA-Ctr/scramble, siRNA-Ctr/anti-miR-101, or EZH2-siRNA/anti-miR-101. The cotransfection efficacy has been tested by (a) EZH2 mRNA and (b) miR-101 levels.

* p value <0.05, as compared with siRNA-Ctr/scramble; ** p value <0.005, as compared with siRNA-Ctr/scramble; # p value <0.05, as compared with siRNA-Ctr/anti-miR-101.

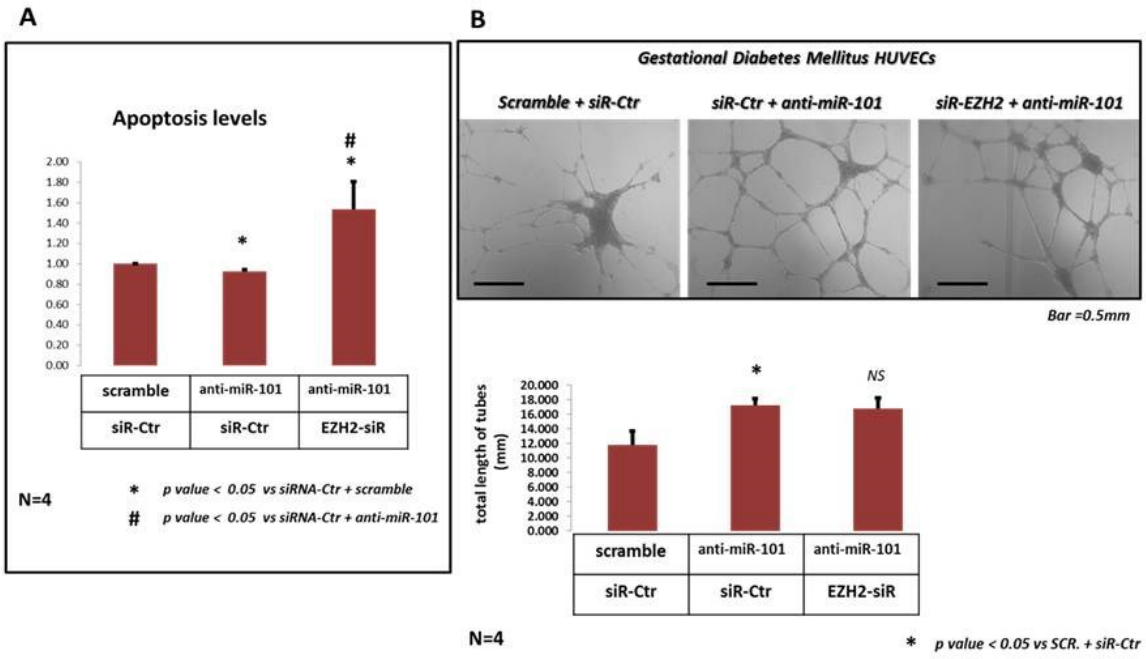

Fig. 24

Effect of the anti-miR-101 with the simultaneously EZH2 inhibition in GDM lineages on apoptosis and on capillary-like tube formation

GDM lineages (N=4) were co-transfected with EZH2-siRNA/anti-miR-101, anti–miR-101/siRNA-Ctr, or scramble/siRNA-Ctr. We analysed the levels of apoptosis (a), calculated in fold change, normalizing to the average of the scramble/siRNA-Ctr, as a control (b) and the angiogenic capacity *in vitro* by matrigel assay. All data are expressed as mean SEM. * p value < 0.05 as compare with scramble/siRNA-Ctr. NS, not significant p value.

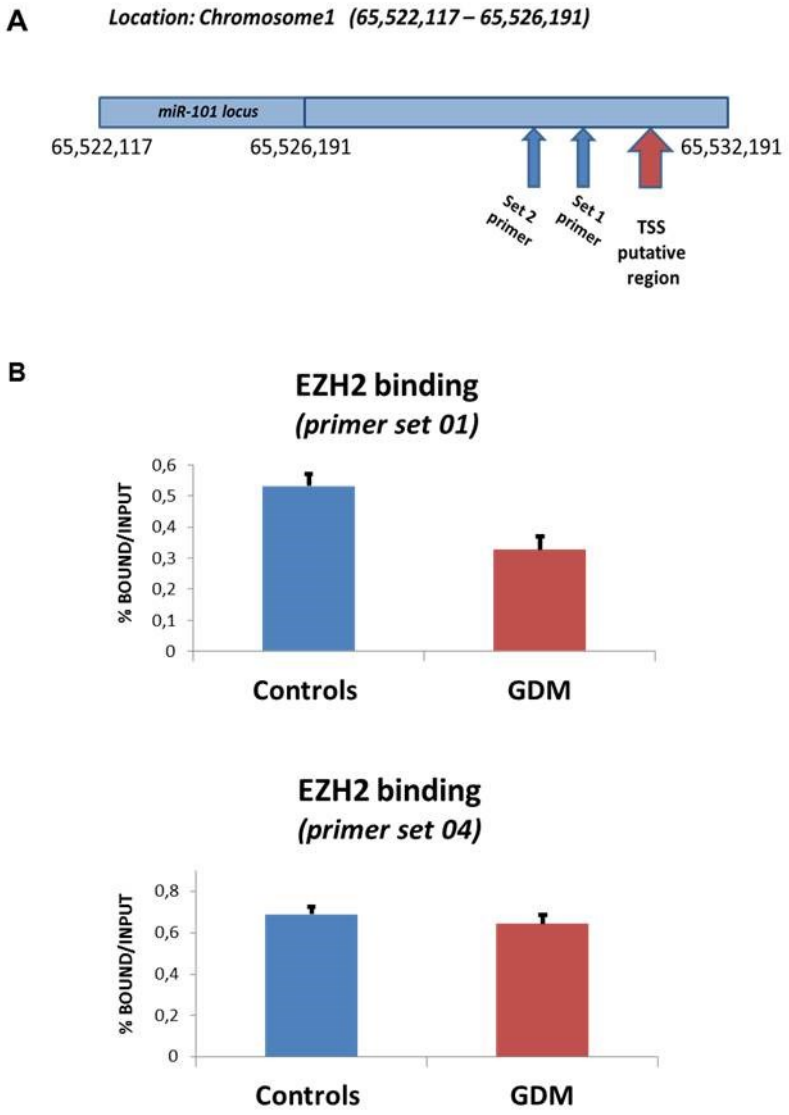

Fig. 25

Scheme showing the location of the *miR-101 locus*, the set of primers used for ChIP and the EZH2occupancy on putative regulatory sequences in 'healthy' and GDM-HUVECs

MiR-101-1 gene is located in the chromosome 1, (chr1: 65,524,117-65,524,191, [-]) and is negative-strand transcribed. (a) In the figure are indicated the transcription starting site (TSS) putative region and the regions amplified by the two set of primers used for the ChIP experiment. (b) The graphs show the EZH2 occupancy on putative regulatory regions of

miR-101 locus in 'healthy' and GDM-derived-HUVECs. We found a tendency toward lower EZH2 occupancy in GDM-HUVECs compared to the controls.

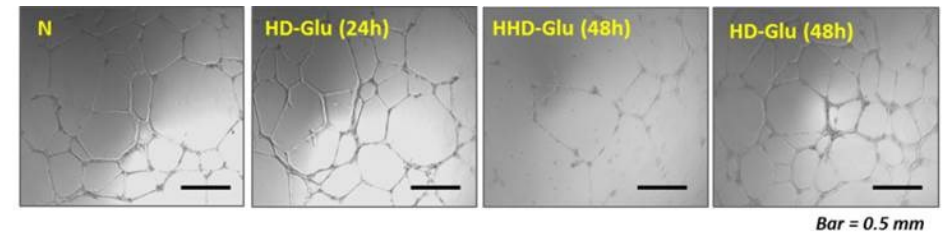

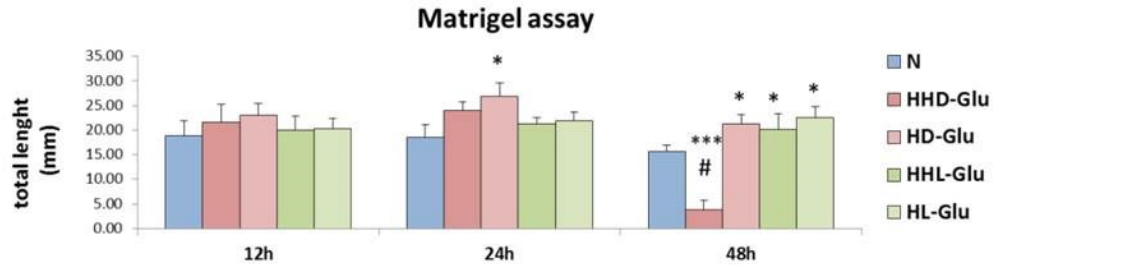

	12h	24h	48h
N	18.8 ± 3.15	18.56 ± 2.54	15.7 ± 1.19
HHD-Glu	21.5 ± 3.79	23.92 ± 1.88	3.85 ± 1.8
HD-Glu	23.09 ± 2.35	26.9 ± 2.63	21.24 ± 2.01
HHL-Glu	20 ± 2.9	21.25 ± 1.31	20.15 ± 3.21
HL-Glu	20.31 ± 2.04	21.83 ± 1.76	22.53 ± 2.2

Fig. 26

Long exposure to D-Glucose impairs the angiogenic capacity of HUVECs *in vitro*

Graph and representative images of the effect of glucose on angiogenic capacity in human umbilical vein endothelial cells (HUVECs) exposed to control level (5.5 mM = N) and high levels of D-glucose (25 mM and 12.5 mM, respectively HHD-glu and HD-glu) and L-glucose, used as osmotic control (HHL-glu and HL-glu), at different time periods (12, 24, 48h). Data

are presented as mean SEM (n = 3). * p value < 0.05, as compared with control group. # p value 0.05, as compared with the group of high L-glucose.

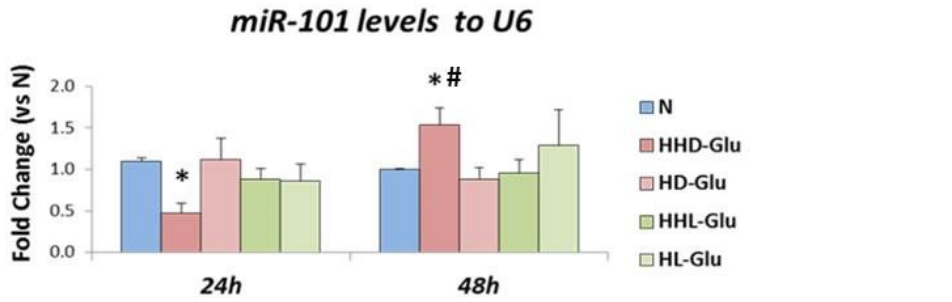

	24h	48h
N	1.09 ± 0.04	1.00 ± 0.002
HHD-Glu	0.46 ± 0.12	1.53 ± 0.21
HD-Glu	1.11 ± 0.26	0.87 ± 0.14
HHL-Glu	0.87 ± 0.13	0.95 ± 0.16
HL-Glu	0.86 ± 0.19	1.29 ± 0.42

Fig. 27

MiR-101 levels in high glucose treated HUVECs (from healthy donors)

'Healthy' HUVECs were cultured in high glucose to mimic the diabetic hyperglycaemia (as specified in the methods) for 24 and 48hours. MiR-101 decreased after 24hours with 25mM of D-glucose compared to the normal and osmotic controls (P<0.05). Then, after 48hours miR-101 increased, as in GDM-extracted HUVECs (P<0.05 compare with normal control –N and osmotic control).

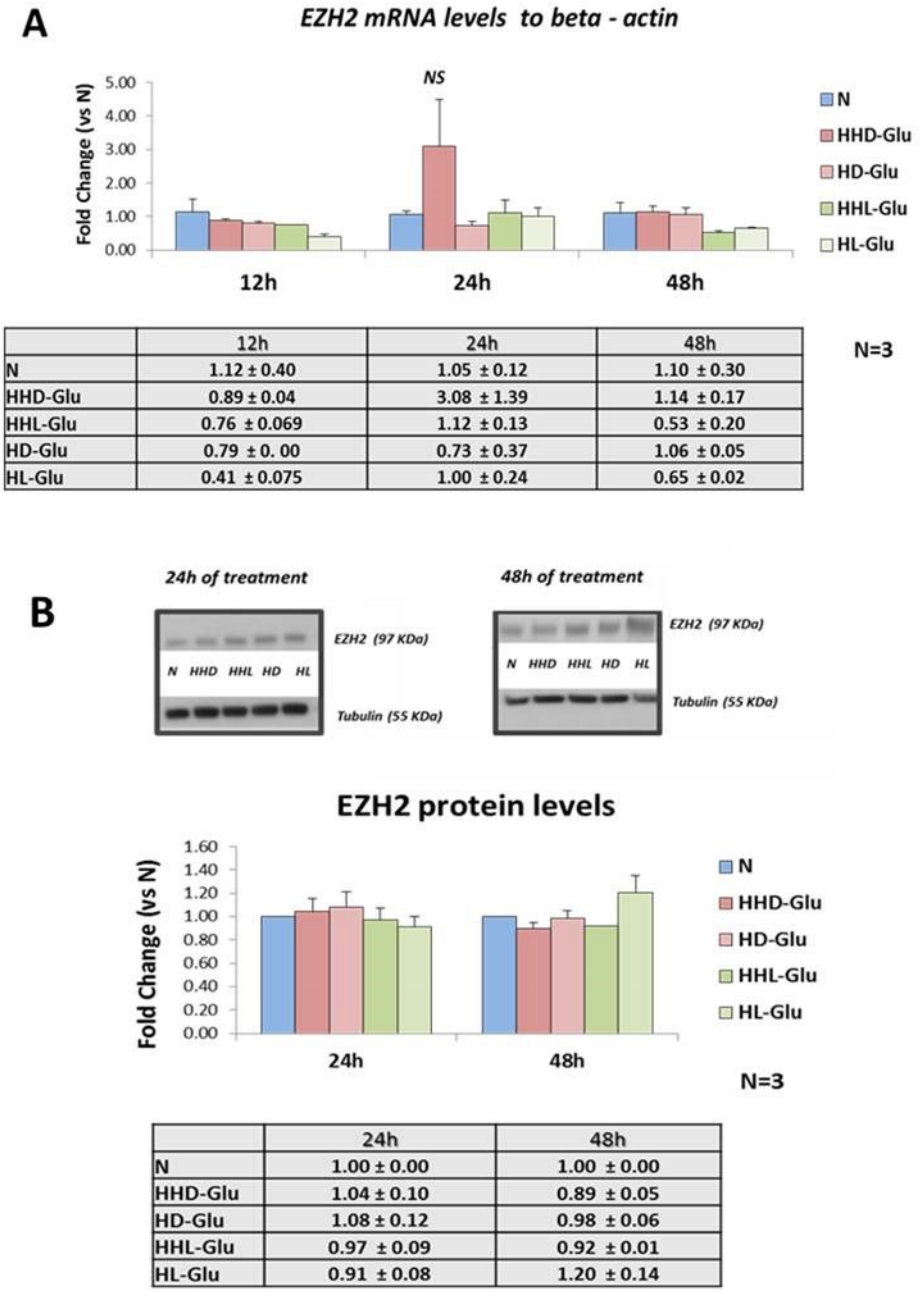

	12h	24h	48h
N	1.12 ± 0.40	1.05 ± 0.12	1.10 ± 0.30
HHD-Glu	0.89 ± 0.04	3.08 ± 1.39	1.14 ± 0.17
HHL-Glu	0.76 ± 0.069	1.12 ± 0.13	0.53 ± 0.20
HD-Glu	0.79 ± 0. 00	0.73 ± 0.37	1.06 ± 0.05
HL-Glu	0.41 ± 0.075	1.00 ± 0.24	0.65 ± 0.02

	24h	48h
N	1.00 ± 0.00	1.00 ± 0.00
HHD-Glu	1.04 ± 0.10	0.89 ± 0.05
HD-Glu	1.08 ± 0.12	0.98 ± 0.06
HHL-Glu	0.97 ± 0.09	0.92 ± 0.01
HL-Glu	0.91 ± 0.08	1.20 ± 0.14

Fig. 28

EZH2 (mRNA and protein levels) evaluated in 'healthy' HUVECs treated with high glucose

In the figure are showed the EZH2 mRNA levels (a) and EZH2 protein levels (b) normalized to tubulin analysed by western blot. Briefly HUVECs

were treated with 12.5mM and 25mM of D-/L- glucose for 24 and 48h, as specified in the methods. Data are presented as mean SEM (n = 3).

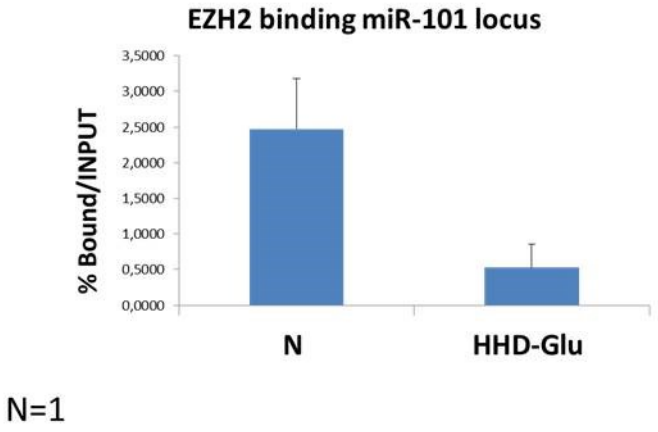

Fig. 29

EZH2 occupancy at the miR-101 regulatory region in high glucose treated HUVECs

Only one 'Healthy' HUVECs lineage were exposed for 48 hours to high or normal concentration of D-Glucose, then fixed, as specified in the methods, and prepared for the chromatin immunoprecipitation. The graph in the figure describes the occupancy of EZH2 on the *miR-101 locus* regulatory region. It shows that the EZH2 binding is lesser in those cells treated with high glucose compare with the normal control. (*Preliminary Data*)

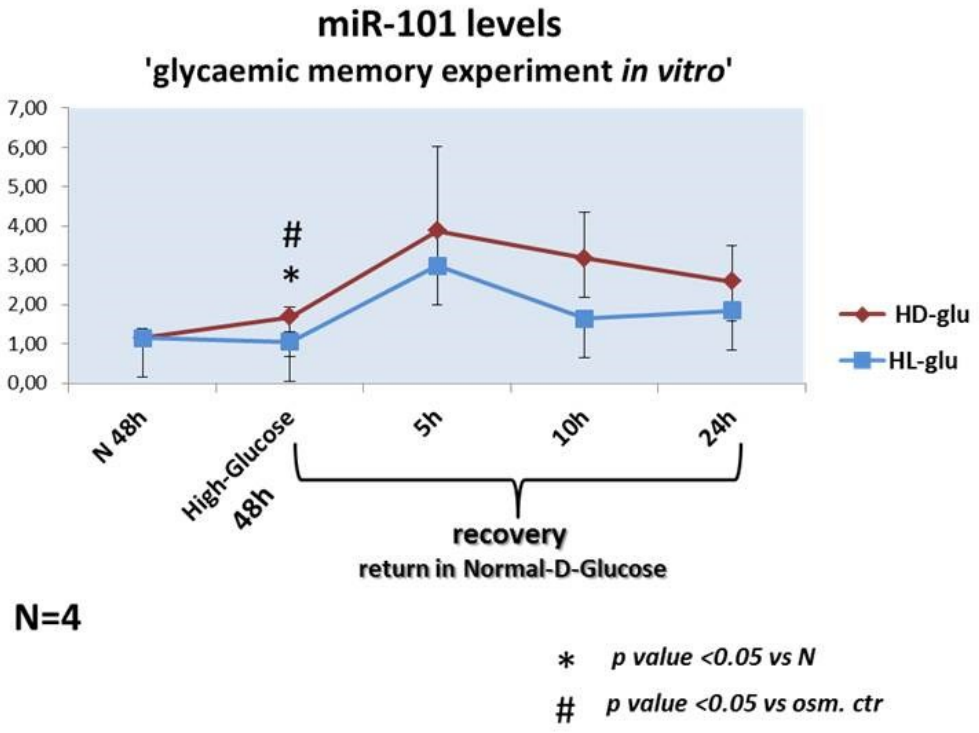

Fig. 30

The 'glyceamic memory' *in vitro*

We performed the "glyceamic memory" experiment culturing 'healthy' HUVECs with 25mM of D-Glucose for 48h, then in normal D-glucose for 5, 10 and 24 hours. The graph shows that miR-101 levels, as previously described, increased in those cells exposed for 48 hours to 25mM of D-glucose then, if return to normal glucose, miR-101 tends to higher levels compared to the normal control, but without any statistical significance.

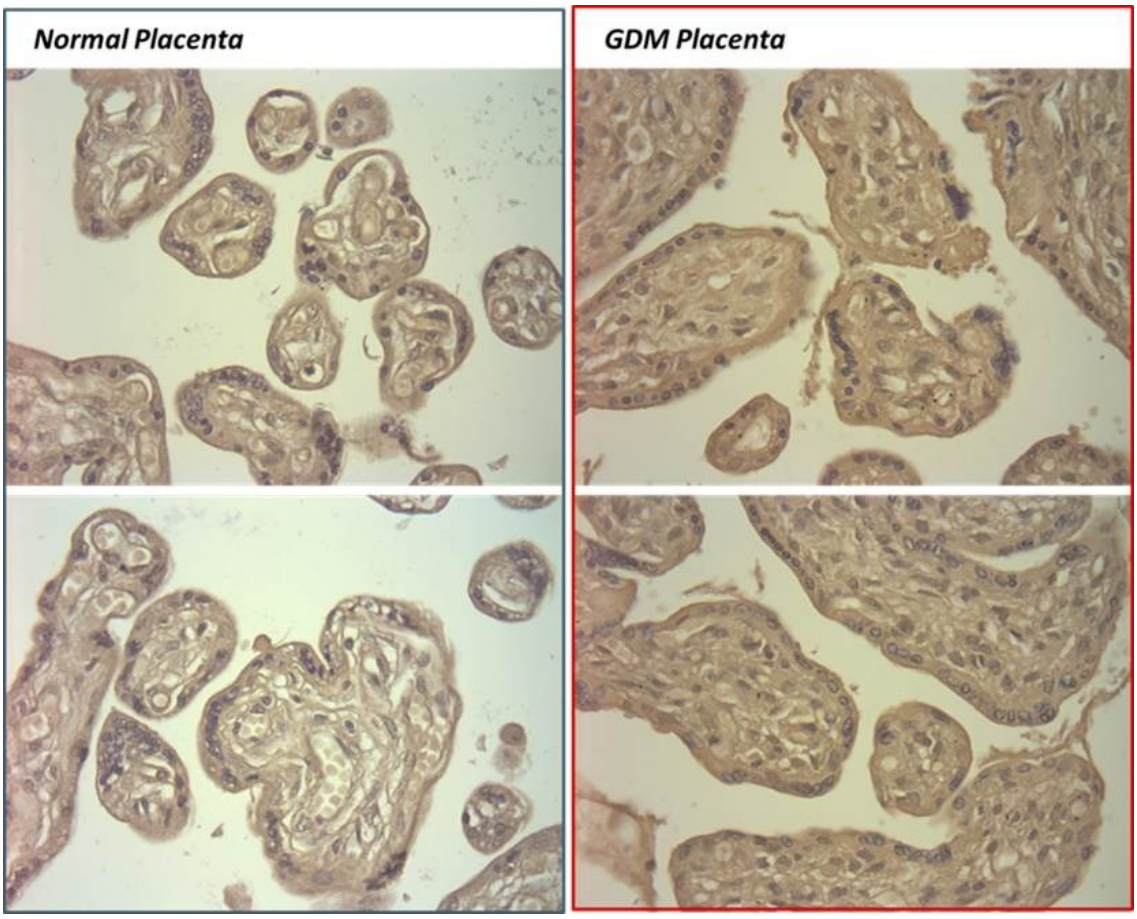

Fig. 31

Hematoxylin-Eosin staining of placenta from 'healthy' and GDM mothers

The Hematoxylin-Eosin staining showed that the mesenchymal tissue of intermediate villi appears denser and more intensely stained in GDM derived placenta than in normoglycemic women. The mesenchyme of the normal placenta has a loose arrangement, with numerous capillaries, while the placenta of women with GDM showed very dense mesenchyme, with fewer villous capillaries. (*Preliminary Data*)

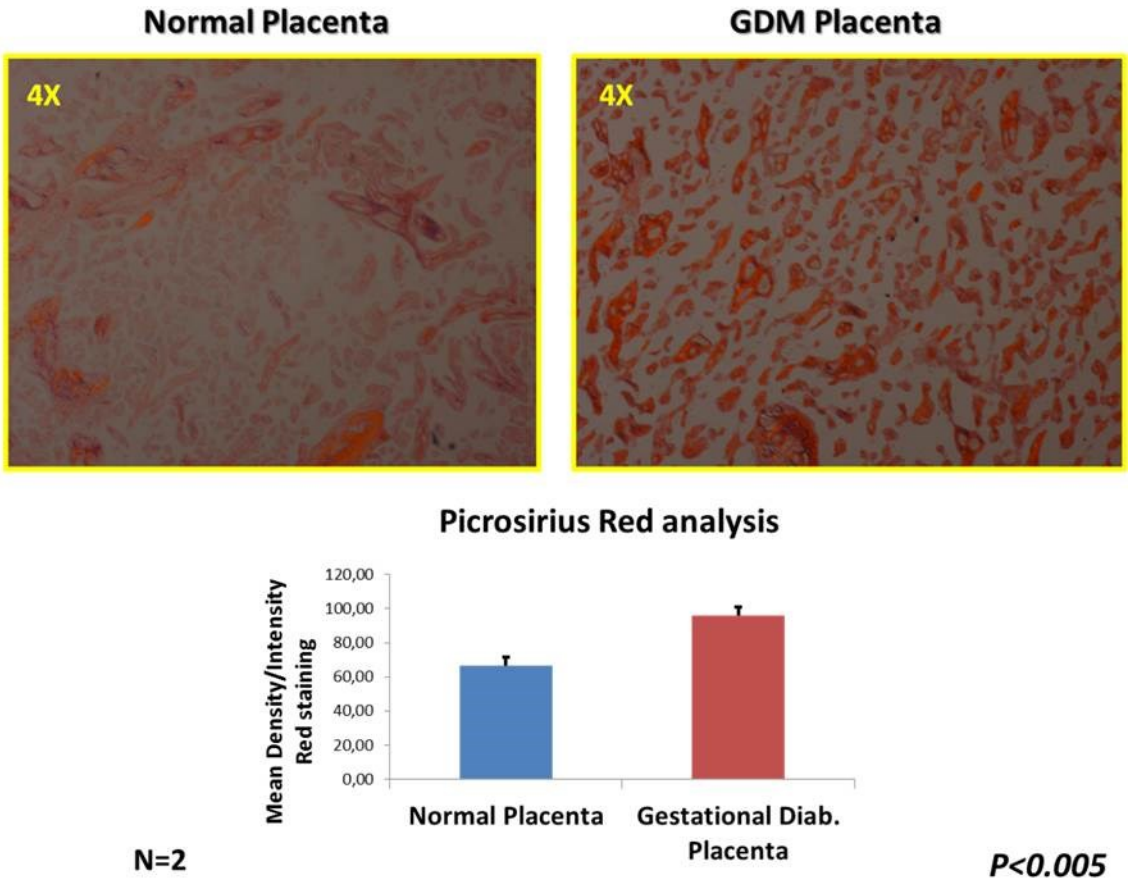

Fig. 32

Picrosirius Red staining of placenta tissue from 'healthy' and GDM donors

The figure Picrosirius Red staining reveals a greater condensation of collagen material around the vessels and villous stroma in placentas of women with gestational diabetes in comparison with the placentas of 'healthy' donors (N=2). The quantification has been performed analysing the mean of density/intensity of the red staining. (*Preliminary Data*)

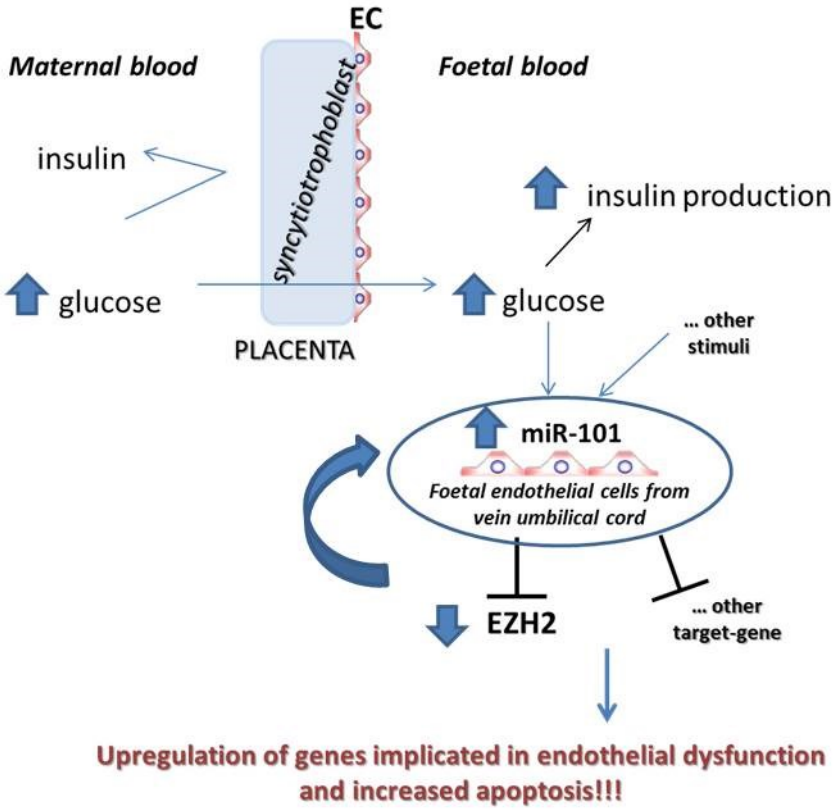

Fig. 33

Summary

We propose that the chronic hyperglyceamia *in utero* leads to conserved "glyceamic memory" in culture. In our study, GDM-HUVECs have higher miR-101 levels compare with the controls, and reduced levels of the target-gene EZH2, both mRNA and protein levels. Moreover, lower EZH2 de-repress the miR-101 transcription stabilising the upregulation of miR-101. These molecular changes, accompanied by phenotypic alteration *in vitro*, were present after 5-6 passage in culture in normal D-Glucose condition. Therefore, are persistent alterations due to the precedent hyperglycaemic environment, conserved "memory" of the cells, even if cultured in normal D-glucose.

REFERENCES

1. American Diabetes Association, "Diagnosis and classification of diabetes mellitus," Diabetes Care, vol. 34, supplement 1, pp. S62–S69, 2011

2. "Diagnosis and classification of diabetes mellitus," Diabetes Care, vol. 33, supplement 1, pp. S62–S69, 2010

3. J. L. Nold and M. K. Georgieff, "Infants of diabetic mothers," Pediatric Clinics of North America, vol. 51, no. 3, pp. 619–637, 20047.

4. M. Catalano and S. Hauguel-De Mouzon, "Is it time to revisit the Pedersen hypothesis in the face of the obesity epidemic?" American Journal of Obstetrics and Gynecology, vol. 204, no. 6, pp. 479–487, 2011

5. J. Pedersen, Diabetes and pregnancy: blood sugar of newborn infants, Ph.D. thesis, Danish Science Press, Copenhagen, Denmark, 1952

6. L. Sobrevia, F. Abarz´ua, J. K. Nien et al., "Review: differential placental macrovascular and microvascular endothelial dysfunction in gestational diabetes," Placenta, vol. 25, pp. S159– S164, 2011

7. M. F. Greene and C. G. Solomon, "Gestational diabetes mellitus—time to treat," New England Journal of Medicine, vol. 352, no. 24, pp. 2544–2546, 2005

8. G. Desoye and S. Hauguel-De Mouzon, "The human placenta in gestational diabetes mellitus: the insulin and cytokine network," Diabetes Care, vol. 30, supplement 2, pp. S120–S126, 2007

9. B. E. Metzger, B. L. Silverman, N. Freinkel, S. L. Dooley, E. S. Ogata, and O. C. Green, "Amniotic fluid insulin concentration as a predictor of

obesity," Archives of Disease in Childhood, vol. 65, no. 10, pp. 1050–1052, 1990

10. J. L.Nold andM. K. Georgieff, "Infants of diabetic mothers," Pediatric Clinics of North America, vol. 51, no. 3, pp. 619–637, 2004

11. M. F. Greene and C. G. Solomon, "Gestational diabetes mellitus—time to treat," New England Journal of Medicine, vol. 352, no. 24, pp. 2544–2546, 2005

12. L. Sobrevia, F. Abarz ´ ua, J. K. Nien et al., "Review: differential placental macrovascular and microvascular endothelial dysfunction in gestational diabetes," Placenta, vol. 25, pp. S159– S164, 2011

13. L. Leach, "Placental vascular dysfunction in diabetic pregnancies: intimations of fetal cardiovascular disease?" Microcirculation, vol. 18, no. 4, pp. 263–269, 2011

14. I. Asmussen, "Ultrastructure of human umbilical arteries. Studies on arteries from newborn children delivered by nonsmoking, White group D, diabetic mothers," Circulation Research, vol. 47, no. 4, pp. 620–626, 1980

15. Nicholas M. Mordwinkin, Joseph G. Ouzounian, Larisa Yedigarova, Martin N. Montoro, Stan G. Louie, Kathleen E. Rodgers "Alteration of endothelial function markers in women with gestational diabetes and their foetuses" The Journal of Maternal-Fetal and Neonatal Medicine, 2012

16. F. M. Stewart, D. J. Freeman, J. E. Ramsay, I. A. Greer, M. Caslake, and W. R. Ferrell, "Longitudinal assessment of maternal endothelial function and markers of inflammation and placental function throughout pregnancy in lean and obese mothers," Journal of Clinical Endocrinology and

Metabolism, vol. 92, no. 3, pp. 969–975, 2007

17. Calles-Escandon J, Cipolla M. Diabetes and endothelial dysfunction: a clinical perspective. Endocr Rev 2001;22:36-52

18. Meigs JB, Hu FB, Rifai N, Manson JE. Biomarkers of endothelial dysfunction and risk of type 2 diabetes mellitus. JAMA 2004;291:1978-1986

19. Hod M, Yogev Y. Goals of metabolic management of gestational diabetes: is it all about the sugar? Diabetes Care 2007;30 Suppl 2:S180-187

20. Nicholas M. Mordwinkin, Joseph G. Ouzounian, Larisa Yedigarova, Martin N. Montoro, Stan G. Louie, Kathleen E. Rodgers "Alteration of endothelial function markers in women with gestational diabetes and their foetuses" The Journal of Maternal-Fetal and Neonatal Medicine, 2012

21. R. Figueroa, E. Martinez, R. P. Fayngersh, N. Tejani, K. M. Mohazzab-H, and M. S. Wolin, "Alterations in relaxation to lactate and H2O2 in human placental vessels from gestational diabetic pregnancies," American Journal of Physiology, vol. 278, no. 3, pp. H706–H713, 2000

22. F. Westermeier, C. Salom´on, M. Gonz´alez et al., "Insulin restores gestational diabetes mellitus-reduced adenosine transport involving differential expression of insulin receptor isoforms in human umbilical vein endothelium," Diabetes, vol. 60, no. 6, pp. 1677–1687, 2011

23. M. Farıas, C. Puebla, F. Westermeier et al., "Nitric oxide reduces SLC29A1 promoter activity and adenosine transport involving transcription factor complex hCHOP-C/EBPα in human umbilical vein endothelial cells from gestational diabetes," Cardiovascular Research, vol. 86, no. 1, pp. 45–54, 2010

24. [no authors listed] The effect of intensive treatment of diabetes on the development and progression of long-term complications in insulin-dependent diabetes mellitus. The Diabetes Control and Complications Trial Research Group. N Engl J Med 1993: 329: 977–986.

25. [no authors listed] Epidemiology of Diabetes Interventions and Complications (EDIC). Design, implementation, and preliminary results of a long-term follow-up of the Diabetes Control and Complications Trial cohort. Diabetes Care 1999: 22: 99–111.

26. [no authors listed] Retinopathy and nephropathy in patients with type 1 diabetes four years after a trial of intensive therapy. The Diabetes Control and Complications Trial/Epidemiology of Diabetes Interventions and Complications Research Group. N Engl J Med 2000: 342: 381–389.

27. Engerman RL, Kern TS. Progression of incipient diabetic retinopathy during good glycemic control. Diabetes. 1987;36:808–12.

28. Hammes HP, Klinzing I, Wiegand S, et al. Islet transplantation inhibits diabetic retinopathy in the sucrose-fed diabetic Cohen rat. Invest Ophthalmol Vis Sci. 1993;34:2092–6.

29. El-Osta A, Brasacchio D, Yao D, et al. Transient high glucose causes persistent epigenetic changes and altered gene expression during subsequent normoglycemia. J Exp Med. 2008;205:2409–17.

30. Brasacchio D, Okabe J, Tikellis C, et al. Hyperglycemia induces a dynamic cooperativity of histone methylase and demethylase enzymes associated with gene-activating epigenetic marks that coexist on the lysine tail. Diabetes. 2009;58:1229–36.

31. Ihnat MA, Thorpe JE, Kamat CD, et al. "Reactive oxygen species mediate a cellular 'memory' of high glucose stress signaling", Diabetologia. 2007;50:1523–31.

32. van Rooij E. "The art of microRNA research", Circ Res 2011; 108:219–234.

33. Wang XH, Qian RZ, Zhang W, Chen SF, Jin HM, Hu RM. "MicroRNA-320 expression in myocardial microvascular endothelial cells and its relationship with insulin-like growth factor-1 in type 2 diabetic rats", Clin Exp Pharmacol Physiol 2009; 36:181–188.

34. Cao, R., Wang, L.J., Wang, H.B., Xia, L., Erdjument-Bromage, H., Tempst, P., Jones, R.S., and Zhang, Y. 2002. "Role of histone H3 lysine 27 methylation in polycomb-group silencing," Science 298: 1039–1043.

35. van der Vlag, J. and Otte, A.P. 1999. "Transcriptional repression mediated by the human polycomb-group protein EED involves histone deacetylation," Nat. Genet. 23: 474–478.

*36. Tzatsos A, Pfau R, Kampranis SC and Tsichlis PN. Ndy1/KDM2B immortalizes mouse embryonic fibroblasts by repressing the Ink4a/Arf locus. Proc Natl Acad Sci U S A. 2009 **8**: 2641–2646.*

*37. Tzatsos A, Paskaleva P, Lymperi S, et al. Lysine-specific Demethylase 2B (KDM2B)-let-7-Enhancer of Zester Homolog 2 (EZH2) Pathway Regulates Cell Cycle Progression and Senescence in Primary Cells. J. Biol. Chem. 2011; **286**:33061-33069.*

*38. Gil J, Bernard D, Peters G. Role of polycomb group proteins in stem cell self-renewal and cancer. DNA Cell Biol. 2005; **24**:117–125.*

*39. Lee TI, Jenner RG, Boyer LA,et al., Control of developmental regulators by Polycomb in human embryonic stem cells. Cell. 2006; **125**:301–313.*

40. Smits M, Mir SE, Nilsson RJ, van der Stoop PM, Niers JM, Marquez VE, Cloos J, Breakefield XO, Krichevsky AM, Noske DP, Tannous BA, Würdinger T. "Down-regulation of miR-101 in endothelial cells promotes blood vessel formation through reduced repression of EZH2" PLoS ONE. 2011;6:e16282.

41. Lu C, Bonome T, Li Y, Kamat AA, Han LY, Schmandt R, Coleman RL, Gershenson DM, Jaffe RB, Birrer MJ, Sood AK. Gene alterations identified by expression profiling in tumor-associated endothelial cells from invasive ovarian carcinoma. Cancer Res. 2007;67:1757–1768.

42. Henryk Dreger, Antje Ludwig, Andrea Weller, Verena Stangl, Gert Baumann, Silke Meiners, Karl Stanglanalyze "Epigenetic Regulation of Cell Adhesion and Communication by Enhancer of Zeste Homolog 2 in Human Endothelial Cells" , Hypertension. 2012.

43. Lu, C., Han, H.D., Mangala, L.S., Ali-Fehmi, R., Newton, C.S., Ozbun, L., Armaiz-Pena, G.N., Hu, W., Stone, R.L., Munkarah, A., et al. (2010). Regulation of tumor angiogenesis by EZH2. Cancer Cell 18, 185–197.

44. Tan, J., Yang, X., Zhuang, L., Jiang, X., Chen, W., Lee, P.L., Karuturi, R.K., Tan, P.B., Liu, E.T., and Yu, Q. (2007). Pharmacologic disruption of Polycombrepressive complex 2-mediated gene repression selectively induces apoptosis in cancer cells. Genes Dev. 21, 1050 1063.

45. Filippos Kottakis, Christos Polytarchou, Parthena Foltopoulou, Ioannis Sanidas, Sotirios C. Kampranis and Philip N. Tsichlis (2011) "FGF-2

Regulates Cell Proliferation, Migration, and Angiogenesis through an NDY1/KDM2B-miR-101-EZH2 Pathway" Mol Cell 43 285–298

46. Varambally, S., Cao, Q., Mani, R.S., Shankar, S., Wang, X., Ateeq, B., Laxman, B., Cao, X., Jing, X., Ramnarayanan, K., et al. (2008). "Genomic loss of microRNA-101 leads to overexpression of histone methyltransferase EZH2 in cancer". Science 322, 1695–1699.

47. Schrauder MG, Fasching PA, Haberle L, Lux MP, Rauh C, Hein A, Bayer CM, Heusinger K, Hartmann A, Strehl JD, Wachter DL, Schulz Wendtland R, Adamietz B, Beckmann MW, Loehberg CR. "Diabetes and prognosis in a breast cancer cohort", J Cancer Res Clin Oncol. 2011; 137:975-983

48. McFarland MS, Cripps R. "Diabetes mellitus and increased risk of cancer: focus on metformin and the insulin analogs", Pharmacotherapy. 2010; 30:1159-1178

49. Wotton CJ, Yeates DG, Goldacre MJ. "Cancer in patients admitted to hospital with diabetes mellitus aged 30 years and over: record linkage studies", Diabetologia 2011;54:527-534.

50. Turner EL, Lane JA, Donovan JL, Davis MJ, Metcalfe C, Neal DE, Hamdy FC, Martin RM. "Association of diabetes mellitus with prostate cancer: nested case- control study (prostate testing for cancer and treatment study)", Int J Cancer. 2011; 128:440-446.

51. Jirkovska M, Kubinova L, Jancek J, Moravcova M, Krejci V, Karen P. "Topological properties and spatial organization of villous capillaries in normal and diabetic placentas. J Vasc Res 2002;39:268e78.

52. Calderon IMP, Damasceno DC, Amorin RL, Costa RAA, Brasil MAM, Rudge MVC. "Morphometric study of placental villi and vessels in women with mild hyperglycemia or gestational or overt diabetes. Diabetes Res Clin Pract 2007;78:65e71.

53. Hull RL, Westermark GT, Westermark P, Kahn SE. Islet amyloid: a critical entity in the pathogenesis of type 2 diabetes. J Clin Endocrinol Metab 2004;89:3629e43.

54. Butler AE, Jang J, Gurlo T, Carty MD, Soeller WC, Bulter PC. "Diabetes due to a progressive defect in beta-cell mass in rats transgenic for human islet amyloid polypeptide (HIP Rat): a new model for type 2 diabetes" Diabetes 2004;53:1509e16.

55. L. Pietro, S. Daher, M.V.C. Rudge, I.M.P. Calderon, D.C. Damasceno, Y.K. Sinzato, C. Bandeira, E. Bevilacqua. "Vascular endothelial growth factor (VEGF) and VEGF-receptor expression in placenta of hyperglycemic pregnant women" Placenta 31 (2010) 770-780.

54. Junqueira LC, Bignolas G, Brentani RR. "Picrosirius staining plus polarization microscopy, a specific method for collagen detection in tissue sections". Hist Jahrb 1979;11:447e55.

55. Lehle K, Haubner F, Mu¨ nzel D, Birnbaum DE, Preuner JG. "Development of a disease-specific model to evaluate endothelial dysfunction in patients with diabetes mellitus", Biochem Biophys Res Commun 2007; 357:308–313.

56. Caporali A, Emanueli C. MicroRNA-503 and the extended microRNA-16 family in angiogenesis. Trends Cardiovasc Med. 2011 6:162–166.

57. Caporali A, Meloni M, Völlenkle C, et al. Deregulation of microRNA-503 contributes to diabetes mellitus-induced impairment of endothelial function and reparative angiogenesis after limb ischemia. Circulation. 2011; 3:282-91.

58. Spinetti G, Fortunato O, Caporali A, et al. MicroRNA-15a and MicroRNA-16 Impair Human Circulating Proangiogenic Cell Functions and Are Increased in the Proangiogenic Cells and Serum of Patients With Critical Limb Ischemia. Circ Res. 2013; 2:335-46.

59. Seki Y, Williams L, Vuguin PM, Charron MJ. Minireview: epigenetic programming of diabetes and obesity: animal models. Endocrinology 2012; 153:1031–1038.

60. Bouchard L, Hivert MF, Guay SP, St-Pierre J, Perron P, Brisson D. Placental adiponectin gene DNA methylation levels are associated with mothers' blood glucose concentration. Diabetes 2012; 61: 1272–1280.

61. Adrian P, Bracken, Pasini D, et al. "EZH2 is downstream of the pRB-E2F pathway, essential for proliferation and amplified in cancer", The EMBO Journal 2003; 22:5323-5335.

62. Hamuro M, Polan J, Natarajan M, Mohan S. High glucose induced nuclear factor kappa B mediated inhibition of endothelial cell migration. Atherosclerosis 2002; 162: 277–287.

63. Facchiano F, Lentini A, Fogliano V, et al. Sugar-induced modification of fibroblast growth factor 2 reduces its angiogenic activity in vivo. Am. J. Pathol. 2002; 161:531–541.

64. Teixeira AS, Andrade SP. Glucose-induced inhibition of angiogenesis in the rat sponge granuloma is prevented by aminoguanidine. Life Sci. 1999; 64:655–662.

65. McGinn S, Saad S, Poronnik P, Pollock CA. High glucose-mediated effects on endothelial cell proliferation occur via p38 MAP kinase. Am J Physiol Endocrinol Metab 2003; 285:E708–E717.

66. Shigematsu S, Yamauchi K, Nakajima K, Iijima S, Aizawa T, Hashizume K. D-Glucose and insulin stimulate migration and tubular formation of human endothelial cells in vitro. Am J Physiol Endocrinol Metab 1999; 277: E433–E438.

67. Zhang J, Han C, Zhu H, Song K, Wu T. miR-101 Inhibits Cholangiocarcinoma Angiogenesis through Targeting Vascular Endothelial Growth Factor (VEGF). Am J Pathol. 2013:182:1629-1639.

68. Mishra R, Singh SK. HIV-1 Tat C modulates expression of miRNA-101 to suppress VE cadherin in human brain microvascular endothelial cells. J Neurosci. 2013:33:5992–6000.

69. Chen K, Fan W, Wang X, Ke X, Wu G, Hu C. MicroRNA-101 mediates the suppressive effect of laminar shear stress on mTOR expression in vascular endothelial cells. Biochem Biophys Res Commun. 2012:427:138-42.

ACKNOWLEGEMENT

I would like to thank both my Supervisors Professor Costanza Emanueli and Professor Gianfranco Pintus for the help and the constant inputs during the research progress.

I would like to thank all the people in the laboratories of Vascular Pathology and Regeneration, Experimental Cardiovascular Medicine School of Clinical Sciences in Bristol and in the laboratory of Vascular Biology in Sassari.

I also thank important collaborators in Sassari for permitting the donors to allow us the use of their tissues for the research, Professor Salvatore Dessole and Gianpiero Capobianco for the umbilical cords and Professor Pasquale Bandiera for providing me the placenta tissues.

With my profound gratitude I also thank my parents, my brother Giuseppe and my sister Chiara for the indispensable encouragement and support.

Finally, a special thanks to my love Jeremy, crucial for the completion of my work and more for having complete my life.